Carrier Profile & Achievements

Prof.(Dr.) Radheshyam Saha, DoB: 15-12-1954,
Caste - General
Res:C-105 Bhrigu Apartments,Sector-9, Plot-4,Dwarka Ph-I,New Delhi – 110077
Tel:011-49094370(R), Mob:+919968291136,
Email:rshahacno@yahoo.com, **rshahacno@gmail.com**

1. Academic Records:

- **Ph. D.** - Electrical Engineering Deptt., IIT Delhi (on FACTS) - 2008
- **M.E.E.** - Electrical Engineering Deptt. , Jadavpur University, Kolkata-1982.
- **B.E.E. (Hons.)** – Electrical Engineering Deptt., Jadavpur University, Kolkata-1980
- **B.Sc. (Hons.)** - Physics Honours, Calcutta University, Kolkata- 1974.

2. Institutional Membership:

- Senior Member of IEEE (USA),
- Life member of IIPA (India)
- Ex-Secretary and Ex-Treasurer, IEEE PELS-IES Delhi Chapter
- Appointed as National Expert in the National Committee on Transmission (NCT) by Ministry of Power, Govt. of India for 2 years upto 22-7-2023 or till further order (vide MoP order dated 23rdh July, 2021).

3. Research Publication:

- **Carried out research on the Power Electronics based Flexible Alternating Current Transmission System Technologies (FACTS) in the Electrical Engineering Deptt., IIT Delhi - Developed 8 new topologies for development of ± 100 MVAr rating STATCOM (Static Synchronous Compensator).**
- **Published 22 research Papers in IEEE / IET International/National Conferences/Journals, etc. and enlisted the same at Annexure.**
- Guiding PhD research scholars and M.Tech (PSY & PES) students as Supervisor;

4. Brief Employment Profile <November 1982 to December, 2014 >

I. Power Sector : <u>Central Electricity Authority (CEA), Ministry of Power, Govt. of India</u>

- **IES Engineering Service'81 -** Joined CEA in Nov., 1983 as Central Power Engineering Service Cadre (CPES), Group- A Class-I officer, Govt. of India. Superannuated on 31-12-14 as Chief Engineer.

- **Served CEA, the Apex Planning body in the Power sector of the Govt. of India,** for over 31 years at various responsible positions (Asstt. Director, Dy. Director, Director & Chief Engineer) from Nov., 1983 to Dec., 2014. Superannuated as Chief Engineer on 31st December, 2014.

II. IT Sector: MMC, Digital System (R&D) (Mahinder & Mahinder Enterprise)

- System Software Engineer Aug '82 - Nov '83.

III. Present Position and Assignments in Delhi Technological University (DTU):

(a) Professor , Electrical Engineering Deptt (Prior to Dec'17, served as Guest Faculty for 3-consecutive semesters)

(b) **Teaching the B.Tech (Elect.) courses** - (i) Utilization of Electrical Energy and Traction **(UEET)** in 5th & 8th Sem (ii) Renewable Energy Systems **(RES)** in 6th Sem (iii) Engineering Analysis and Design **(EAD)** in 3rd Sem (iv) Numerical and Engineering Optimization Methods **(NEOM)** & Virtual Lab in 3rd Sem (v) Control System **(CS)** in 4th Sem (vi) Power system operation & Control Lab in 6th Sem (vii) Control System Lab in 4th Sem (viii) Automotive Electricals & Electronics Lab in 4th Sem (ix) Basic Electrical Engg. Lab in 2nd Sem, etc.

Teaching M.Tech Course: Energy Management System (EMS),PES.

(c) Faculty Supervisor:

- Role of guiding three PhD students – two full time and one part-time;
- Supervisor of M.Tech (PSY) student 2019 and 2020 batch, and
- Guide for B.Tech final year students (Major-I & Major-II projects) 2018, 2019 & 2020.

(d) Key role in organizing Workshops at EDUSAT, EED, DTU:

- IEEE Workshop on Power Electronics in Smart Grid and Optimal Power Trading Mechanism held on 3rd Nov.,2018;
- IEEE Workshop & Exposition on Grid Integrated Renewables & Electric Transportation, 17-18th Dec.,2019.

(e) Delivered FDP Talks during 2019-20 on the following technical topics:

- "Power System- Cutting Edge Technologies" in DTU in December 2019;
- "Power Quality and Reactive Power Management" (ONLINE) in DTU in July 2020;
- "Power Electronics and Power System" (ONLINE) in O P Jindal University, Raigarh in Aug., 2020.

(f) Chairing Session in IEEE Conference (viz. Chaired session of 2018 2nd IEEE ICPEICES conference held in Oct'18 EED DTU, & other IEEE platforms)

(g) Give Expert Talks (Self) on invitation to organizations viz. NTPC, NVVN, CPRI,DVC, CERC,CU,IPMA etc. on Power System/FACTS

(h) Responsibility in organizing expert lectures at EDUSAT, EED by Industry experts in EED, DTU on contemporary topics and the state-of-the–art technologies under the aegis of IEEE-PELS Delhi Chapter.

Distinguished Speakers from various Industries/Organizations invited :

- Sh. KVS Baba, **Chairman and Managing Director, POSOCO** on 17th Dec'20 on Renewable Energy Integration in India (IEEE Workshop & Exposition).
- Dr Subir Sen, **COO/ED, POWERGRID** on 3rd Nov'18 on "Power Electronics in Smart Grid and Optimal Power Trading Mechanism"
- Sh S L Narasimhan , **Director, POSOCO** on 27th Feb.,2020 on "Grid Codes and Standards and Electricity Markets for successfully integrating Renewable Energy"
- Sh Krishna Sankar Bandopadhaya, **General Manager, NVVN** and Sh Abhay Kr. Srivastava **AGM**, on 3rd November'18 (IEEE Workshop on " Power Electronics in Smart Grid and Optimal Power Trading Mechanism")
- Sh. S.S.Barpanda, **Executive Director, NRLDC** Power System Operation Corporation Limited on "Power Market in India", in December, 2019.

(i) Responsibility of the overall B.Tech Project Coordinator, (Major-I & Major-II) EED, (2019-20 for 238 Students & 2020-21).

(j) Spearheaded the update of Utilization of Electrical Energy (UEE) Manual.

(k) Spearheaded the preparation of Numerical Engineering and Optimization Methods (NEOM) Virtual Lab Manual.

(l) Examination of Industrial training Reports of the B.Tech students

(m) Online summer training for two months for the B. Tech students from June 5 – Aug 10 2020:

"Study on the performance of Indian Grid System during the Blackout Condition on 5th Apr'20 (21:00-21:10hrs)" [GoI initiated Action on Covid Situation]

5. Major Areas of Technical Capabilities and Expertise:

- Research & Development of Power Electronics based FACTS (Flexible AC Transmission systems) Technologies viz. STATCOM, SVC, TCSC etc.
- Designing & Planning of Regional and National Electricity Grids.
- Basic and Advanced Electrical/Power Systems Know-hows & Control System
- System Stability & Security perspectives of integrated Electricity Grid;
- Power System studies, planning, evaluation & optimization using PSS/E, SIMPOW,NEPLAN & IREQ Software packages.
- Integration of Renewable Energy Sources (RES) with Grid.
- Designing of perspective Transmission grid Master Plan as done for Bhutan, Delhi, Sikkim, etc.
- Formulation of Road map for South Asian (SAARC) Electricity Grid
- Real time Power System Control, Operation & Technological up-gradation of electricity grid control mechanisms (viz. SCADA, PMU, PDC, WAN, etc.)
- Electricity Market Mechanism & Economics/ Cross-border electricity trading;
- Consultancy to the Power utilities on Power System Development & capacity Building
- Software Development/Up-gradation (e.g. Operating system, Real time Compiler, Basic Interpreter, etc.)
- Simulation Techniques in the MATLAB platform.

6. Major Milestones Achieved:

- ***Power System Technologies, Planning, Operation & Grid Stability***

  (i) Carried out intensive research in the field of Transmission Technologies- FACTS - Developed 8 new topologies for development of ± 100 MVAr rating STATCOM (Static Synchronous Compensator) as part of Ph. D work.

  (ii) Sphere headed State & Regional Transmission Grid Planning & Development for Southern (SR), Eastern(ER), North East(NER) Regions and all India Perspective Transmission Plan.

  (iii) Planned the comprehensive Transmission and Sub-Transmission system Road Map and related funding modalities for each of the States in NER.

(iv) *Sphere headed the preparation of the* ***Transmission Master Plan for Arunachal Pradesh*** *for harnessing 40,000MW hydro potential from various hydro basins in the State.*

(v) *Responsible of evolving and reviewing* ***Transmission Master Plan of Sikkim*** *for 6000MW hydro Projects at various hydro basins.*

(vi) *Key role in formulating* ***Perspective National Transmission Grid Plan 1999 and 2007*** *aiming at developing National Grid in the country with free flow of power across the regional boundaries.*

(vii) ***Convening Standing Committee meeting on Power System Planning*** *and finalizing transmission system strengthening, evacuation system for IPPs and other generation projects, grid connectivity and long term access (LTA)*

(viii) *Sphere headed the* ***consultancy to Royal Government of Bhutan for planning and evolving of National Transmission grid Master Plan (NTGMP) for Bhutan for 2020 and 2030 scenarios*** *with synchronous operation with Indian Grid, and prepared blue print of the Bhutan National Transmission Grid having seventy-five HEPs with a total generating capacity of about 27000 MW at various river basins.*

(ix) *Sphere headed the preparation of the* ***Transmission Master Plan for Delhi corresponding to 2016-17 and 2021-22 time frames*** *based on comprehensive system studies.*

(x) *Responsible for* ***Cross border Transmission system planning between India and SAARC member States viz. Nepal, Bhutan , Bangladesh ,Sri Lanka and Pakistan; Responsible for cross border bilateral Power Trading/Exchange*** *between India and neighboring South Asian countries(SAARC).*

(xi) *Key role in drafting and finalization of* ***Power Trade Agreement between Govt. of Nepal and Min. of Power, Govt. Of India.***

(xii) ***Participation in the 18th SAARC Summit held from 23-27 November 2014 at Kathmandu, Nepal as one of the Indian Delegates*** *and involvement in the Framework Agreement on SAARC Electricity trade.*

(xiii) *Responsibility for* ***review of intra-State and inter-State Green Energy Corridors for large scale integration of Renewable electricity generation sources being harnessed at various locations/States in India.***

(xiv) *Headed the Task Force on the* ***technical studies with regard to Grid Stability and security and TTC violation in the all India grid during 23-7-12 to 31-7-12 and twin blackouts on 30th and 31st July 2012 in India.***

(xv) *Specialized system studies for* ***Sub-Synchronous Resonance Analysis in series compensated transmission lines*** *associated with large capacity thermal generation Projects (viz. Lalitpur TPS in UP, Jindal TPS in Odisha)*

(xvi) *Responsible for Comprehensive Planning and Appraisal of Bihar T&D system corresponding to 12th Plan and beyond; Trans-country transmission system strengthening between Bihar (India) and Nepal to facilitate additional supply of 175 MW to Nepal.*

(xvii) Assessment of Grid Stability in respect of synchronous operation of Nepal and India Electricity Grids with the commissioning of 400kV Muzaffarpur –Dhalkebar D/C line between the two countries.

(xviii) Responsible for recommending prior approval of Government of India under Section 68 Indian Electricity Act, 2003 for various inter-State Transmission and private sector transmission schemes.

- ***Power System Project Monitoring***

(i) Sphere-headed creation of transmission system data base for scheduling, and monitoring of ***physical construction progress for CTU, STUs ,Private and Cross border's planned transmission elements/projects in the country****.*

(ii) *Initiated various measures to* ***minimize timeline for implementation of projects involving Technical and Physical constraints viz. Forest clearance, RoW issues, Land acquisition, etc.***

(iii) Prioritization of various transmission works (year-ahead basis) for its early implementation viz. inter and intra-regional system strengthening, ATS for generation projects, Cross Border links, and ***formulation of Result Frame Work Document (RFD) for CTU, STUs and Private Developers.***

(iv) Organized meeting with various stakeholders on regular basis to review and monitor the various action plans and physical progress for timely completion of Projects.

- ***Integrated Grid operation and Control - Real time operation***

(i) Undertaken the responsibility of ***Control room shift-in –charge at Eastern Regional Load Dispatch Center (ERLDC)*** *for real time load dispatching, scheduling and control of the Eastern Regional Grid*

(ii) System co-ordination with State power utilities, ***capacity building*** *in central generating and transmission utilities, Power flow Studies, Contingency Planning and optimal system management.*

(iii) Sphere-headed the Preparation of Specification, tender document for procurement of computer systems and power system tools for transmission system planning and operational studies.

- ***Electricity Market Study & Operation***

(i) Study on European Electricity Market Mechanism for cross border trade and power market design of TSOs at Amsterdam and Paris.

7. Professional Visits Abroad: *USA, Netherlands, France, Bhutan, Nepal and Bangladesh.*

8. Major Training Exposures

(i) *SOSYNAUT- SCADA installed at ERLDC/EREB by M/s Siemens for real time operation, control & management of integrated power system (Aug'85-Jan'86 at EREB Kolkata).*

(ii) PSSE / *SIMPOW / NEPLAN /MATLAB Power System Software Packages*

(iii) Technology Improvement Program on Flexible Alternating Current Systems (FACTS) at M/s MWH in USA, Aug 12 – Oct 11, 2001.

(iv) *Study tour at Amsterdam and Paris from 13-19 July 2014 to explore the European Regional Power Market - Evolution process of harmonization of legal, regulatory and policy issues, operational and power market design.*

9. Area of Interests

R&D on Power Electronics based Smart Controllers viz. STATCOM /SVC/ UHVDC/ HVDC light/UHVAC/TCSC/UPFC/IPFC; Power Quality; RES Technologies, Renewable Energy Integration, Optimal Power Balancing, Storage Capacity Planning; Smart Transmission & Distribution Grid; Transmission capacity enhancement & Improvement; Real time Dynamic State Measurements using WAN, Smart Grid and its Stability, Reliability & Security; Synchronous SAARC Electricity Grid & Cross Border Power Exchange/Trading;

Annexure

Papers Published in IEEE / IET International/National Journals / Conferences etc.

1. "Modeling of Harmonic Neutralized 12-Pulse Static compensator(STATCOM)", in proc. of 2006 **IEEE Power India Conference**, India, Apr.8-10, 2006.
2. "A Review on FACTS Devices", **ICFAI Journal of Science & Technology**, Vol.2, No.2, pp. 6-51, Sept. 2006.
3. "Modeling of 18-Pulse STATCOM for Power System Applications", **Journal of Power Electronic Korea (KJPE)**, Vol.7, No.2 pp. 146-158, April 2007.
4. "A New 24-Pulse STATCOM for Voltage Regulation", in proc. **IEEE International Conference** on Power Electronics, Drives and Energy Systems (PEDES) 2006, India, Dec. 12-15.
5. "Static synchronous compensators (STATCOM): a review", **IET Power Electronics Journal**, 2009, Vol. 2, Iss.4, pp. 297-324.
6. "Improved 48-pulse static synchronous compensator for high-voltage applications" **IET Power Electronics Journal**, 2010, Vol. 3, Iss.3, pp. 355-368.
7. "Enhancing Power Transfer Capacity of Transmission System by a Reduced Magnetics based 48-Pulse STATCOM Controller" in Proc. of POWERCON 2008 and **IEEE Power India Conference**.
8. "Three-Level 24-Pulse STATCOM with Optimized Magnetics to Regulate Voltage in Transmission System" in **Int. Journal of Power Electronics (IJPELEC),** Vol.3, No.2, 2011, pp. 134-155.
9. "Analysis of a Harmonics Neutralized 48-Pulse STATCOM with GTO Based Voltage Source Converters" in **Journal of Electrical Engineering & Technology**, Vol.3 No.3, pp.391-400, 2008.
10. "Modeling of Harmonic Optimized 12-Pulse Static Compensator (STATCOM)", **Journal of the Institution of Engineers (India).**
11. "Towards National Power Grid" in the Proce. of Formation of **National Power Grid Conference**, 1992, Hyderabad.
12. "Some Aspects of FACTS and other Technology in Power Transmission Control" in **"Transtech (Workshop on T &D Practices)", DVC**, Aug. 12 2006.
13. New Role of Transformer Magnetics in FACTS Technology" in the Proce. of **10th International Conference on Transformers (TRAFOSEM-2008)** ,11-12th Nov., 2008, India.
14. "A 3x6 Pulse NPC-VSC based ±100 MVAr STATCOM Modeling and Applications",6th **IEEE Power India International Conference** Proc,, PIICON 14, New Delhi, December 5-7 2014.
15. Frequency Regulation Technique in AC-DC Network using Converter Current Modulation in VSC-HVDC System' , **IEEE Conference**, **INDICON**, 11 -13th December, 2020, New Delhi,India

16. ‘An Adaptive Master-Slave Technique using Converter Current Modulation in VSC-based MTDC System’, **IEEE 6th International Conference** for Convergence in Technology (I2CT), 2 - 4 April, 2021, Pune, India.

17. ‘Analysis of Control Techniques for Voltage Source Converters-Based MTDC ‘, **European Power Electronics and Drives Journal**, **Taylor and Francis.** (DoS- July, 2020) - **Acceptance Awaited**

18. “Modelling Financially Motivated Cyber Attacks on Electricity Markets using MILP Program”, **2nd IEEE International conference on power, Energy, control and transmission systems (ICPECTS’20)** , Chennai, India, pp:1-6, 10th-11th December, 2020. (Best Paper Award)

19. “ Two Stage Stochastic programming model for optimal scheduling of RE based Virtual Power Plants in Electricity Markets ”,. **IEEE 6th International Conference for Convergence in Technology (I2CT)**, Pune, India, pp. 1-6, 2nd - 4th April, 2021.

20. “Solar PV based Forest Fire Detection and Monitoring using Zigbee Protocol”, **International conference for Intelligent Technologies (CONIT’21)** ,2 April 2021—Accepted

21. **“**DESIGN AND MODELING OF A FILTER ASSISTED 6-PULSE VSC-IGBT BASED D-STATCOM FOR REACTIVE POWER COMPENSATION”, **“IEEE Sponsored Asian Conference on Innovation in Technology (ASIANCON) 2021”**. Pune, Maharashtra, India.

22. “Bi-level Optimal Strategic Generation Scheduling with Flexible Demands under Uncertainties and Improving Profitability of VPP in Day Ahead and Reserve Electricity Markets” , **International Journal of Electrical Power and Energy Systems, Elsevier (Communicated).**

No. 15/3/2017-Trans
Government of India
Ministry of Power
Shram Shakti Bhavan, New Delhi – 110 001.
****

Dated, 23rd July 2021

OFFICE ORDER

Subject: Nomination of two experts in the "National Committee on Transmission" (NCT)- regarding.

The undersigned is directed to refer to this Ministry's Office Order of even number dated 4.11.2019 and to state that the Competent Authority in the Ministry of Power has approved the nomination of following two experts in the National Committee on Transmission (NCT):

i. Dr. Radheshyam Saha, Ex. Chief Engineer, CEA
ii. Shri Sushanta Kumar Ray Mohapatra, Ex. Chief Engineer, CEA

2. The nomination of above two experts in the NCT shall be for a period of two (2) years i.e till 22.07.2023, or till further order, whichever is early.

(Goutam Ghosh)
Director (Trans)
Tele-fax: 011-23325242
Email: transdesk-mop@nic.in

To

1. Dr. Radheshyam Saha, Ex. Chief Engineer, CEA
2. Shri Sushanta Kumar Ray Mohapatra, Ex. Chief Engineer, CEA
3. Chairperson, CEA
4. All members of NCT.
5. CMDs of all CPSUs and Heads of all autonomous bodies under the Ministry of Power, Govt. of India.
6. Power/ Energy Secretaries of all States/UTs and Chief Executives of all State Power Transmission Utilities.
7. Finance/ Budget Section, Ministry of Power.

Copy to:

1. PS to Minister of Power & NRE
2. PS to Minister of State for Power
3. Sr. PPS/ PPS/ PS to Secretary(Power)/ AS(SKGR)/ AS(VKD)/ AS&FA/ all Joint Secretaries/ Directors/ Dy. Secretaries, Ministry of Power.
4. Technical Director, NIC, MoP- for publishing on MoP website.

Communicated

Analysis of Control Techniques for Voltage Source Converters-Based for MTDC Systems

Ashima Taneja, R. Saha, Madhusudan Singh

Department of Electrical Engineering, Delhi Technological University.

Abstract—VSC-based multi-terminal DC transmission system is increasingly being used in combination with AC grid for evacuation of power from distributed generation, bulk power transfer and for enhancement of grid reliability and security. Various control strategies like Master-Slave control, Voltage Margin Control and Voltage Droop control are adopted for VSC-MTDC systems. This paper attempts to review these control strategies and determine that Voltage droop control in comparison with the other control techniques is much better and reliable option for VSC-based MTDC system. A sensitivity analysis on steady state and dynamic performance has been carried out in MATLAB/Simulink platform for a typical four-terminal VSC-MTDC system interconnected to AC-grid being subjected to load variations, converter terminal outage and three-phase to ground fault. It is validated from the simulation results of many case studies that Voltage Droop control is superior. It is observed also that entire burden of power balancing within the DC grid gets well shared among the droop controllers. But in case of Master-Slave and Voltage Margin techniques, the entire power balancing is shared by a single converter terminal causing severe capacity constraints in specific terminal.

Keywords—Decoupled Vector control, SPWM, Master-Slave, Single and Two-stage Voltage Margin, Voltage Droop.

I. INTRODUCTION

With rapid developments in power electronics and exponential up gradations in power semiconductor ratings, High Voltage Direct Current (HVDC) technology has turn out to be the cost economical choice for remotely located generation and bulk power transmission over a long distance for reliable, flexible and efficient means of power transfer. In addition, better stability of AC-DC grid, rapid control, asynchronous interconnection ability are some of the attributes for laying several miles of HVDC lines [26, 39, 41]. With up gradations in thyristor technology, it has been possible to transfer over 12 GW of power over 3293 kilometers in Changji – Guquan HVDC project in China [41]. However, this technology works reliably with stronger AC networks at its receiving and sending ends to avoid any commutation failures. Also, due to phase control by means of delay angle given to thyristor converter, it needs to be supplemented with huge reactive power supplies at both the ends [40]. An alternative to thyristor-based HVDC transmission systems is self-commutated Voltage Source Converter (VSC) based HVDC technology. It has significant advantages like decoupled control of power, ability to energize passive systems, simpler power flow reversal, etc. and has overcome almost all the limitations of thyristor-based technology [9].

The exploitation of large offshore wind reservoir [42] available provides a significant opportunity for employing VSC-based HVDC transmission systems. Improved power quality, dynamic reactive power support, interconnecting with weak ac systems, smaller footprints, increased reliability, and in certain cases transformer elimination make VSC-HVDC suitable for integrating offshore wind power with the onshore grids [43]. Nonetheless, VSC-HVDC technology has an edge over conventional thyristor based HVDC not only for interconnection of wind farms but also for feeding island loads like offshore platforms or for supplying power to congested urban areas using Multi-terminal HVDC systems [3, 15, 23 32, 43]. It is noted in [24] that transmission of offshore wind power over distances of 150 kms is done by employing underground DC cables and VSC-HVDC technology. It is envisioned that future challenges of the power systems can be met by making interconnection among various AC networks via MTDC grids [25].

The major challenges associated with operation of multi-terminal HVDC systems involve precise control of DC voltage of the grid, power flow balancing and interconnection and sharing of power reserves among the neighboring AC networks. In addition, it requires a reliable and faster acting circuit breaker to isolate DC faults to avoid de- energizing of the entire grid [21, 22, 26]. Research on MTDC systems [36] these days is focused on issues like fault ride through capability of AC and DC systems, enhancement of transient stability, developing combined AC and DC power flow algorithms and proposing various frequency support techniques using power available in the DC grid.

The control of VSC-based MTDC systems has been demonstrated in [8-9,13-23,25-39,43-44] in which Master-slave control, Voltage Margin control and Voltage Droop control has been well explained in [13, 15, 17, 26]. Master-slave enables to keep DC voltage constant but burdens single terminal. The operational reliability of DC grid gets compromised if Master goes into an unscheduled outage. Incorporation of additional voltage controlling terminal with a different reference value by implementing Voltage Margin although increases reliability of MTDC but introduces oscillations; still secure operation of the grid is subjective to matching grid voltage with that of Reserve Master. Voltage Droop controls increases the reliability by having more than one voltage controlling terminals. Also, power flow balance is ensured without burdening a single terminal that too without any requirement to meet any predefined condition for transfer of control among the DC voltage controlling terminals. But, droop-control too suffers from certain operational

Electrical Power Electronics and Drives, Taylor and Francis
Date of Submission: 3rd July, 2020

2020 IEEE 17th India Council International Conference (INDICON) | 978-1-7281-6916-3/20/$31.00 ©2020 IEEE | DOI: 10.1109/INDICON49873.2020.9342451

Frequency Regulation Technique in AC-DC Network using Converter Current Modulation in VSC-HVDC System

Ashima Taneja, Radheshyam Saha, Madhusudan Singh
Department of Electrical Engineering, Delhi Technological University.
tanejaashima88@gmail.com,rsaha@dtu.ac.in and madhusudan@dce.ac.in.

***Abstract*—In order to meet existing and future load growth, capacity addition by economical RE generation and replacement of hydrocarbon-driven or fossil fuel-based alternators are the major trend in power system development worldwide. In effect, there is gradual decrease in system inertia. The intermittency and variability of RE-sources being a well-established phenomenon creates not only load-generation balancing issues in real time scale, but leads to system operational problems like wide frequency fluctuations, high rate of change of frequency, etc. This makes the power system very much prone to serious frequency insecurities. For secure operation of integrated EHVAC-HVDC hybrid power system, frequency regulation concept is embedded inside converter control systems and a telecommunication-independent active power frequency droop-based Converter Current Modulation technique using IGBT-based VSC HVDC system is proposed in this paper, which offers support to maintain stable frequency near nominal value in an interconnected power system during generation loss, load-switching or a fault in the system, avoiding any frequency dip. The proposed VSC- HVDC control scheme has been simulated by MATLAB/Simulink tool and performance of the controller is demonstrated to validate the superiority of the proposed scheme over the conventional vector current control scheme used in VSC-HVDC system.**

Keywords—Vector control, frequency nadir, power-frequency droop, telecommunication-free frequency support.

I. INTRODUCTION

With increase in electricity demand and larger penetration of renewable electricity (RE) generation from location specific predominant wind and solar sources, modern power systems are strongly coupled with AC and DC transmission systems. HVDC transmission system inter-alia provides flexibility of power flow control and enhances power system stability for the well-knit AC-DC grid. In fact, HVDC transmission is a viable alternative for submarine cable power transmission from offshore wind power plants and acts as a firewall in between the interconnected AC networks to prevent any disturbance to propagate from one AC network to other [1,3].

Exponential increase in ratings of power semiconductors like IGBTs has led to widespread popularity of VSC-based HVDC transmission systems. VSC-based HVDC transmission systems overcome various limitations of conventional thyristor-based LCC-HVDC transmission technology like risk of commutation failure when interconnected to weak AC grid, high quantum of reactive power requirement, etc. Also, VSC-based HVDC requires much smaller footprints compared to the LCC-HVDC technology and enables the system operator to obtain the benefits of decoupled active and reactive power flow control, black start capability and faster but simpler power flow reversal [2-4].

It is anticipated that in future electrical power systems, conventional hydrocarbon-based synchronous power generation will be completely replaced by green power generation using abundant natural resources of renewables and modern semiconductor technologies like VSC-HVDC transmission. However, the leading trend of capacity addition by economical RE generation results in an overall decrease in inertia of power systems. The intermittency and variability of RE sources creates load-generation balancing problems like wide frequency fluctuations, high rate of change of frequency (RoCoF), etc. This makes the power systems very much prone to serious frequency instabilities [4]. It is essential to avoid any such volatilities and thus, making it fairly indispensable to include frequency support mechanism in the control strategies of modern VSC-based HVDC transmission systems.

The conventional vector control scheme for VSC-based HVDC transmission systems has been illustrated in [2-4]. It has been shown in [1] that by introducing active power-frequency droop control characteristic in converter control scheme of VSC-based HVDC systems, an increase in amount of coupling between the AC grids of sending and receiving ends is observed. That is, in response to occurrence of a frequency disturbance event e.g. generation loss, sudden load switching or fault, in any of the two grids, healthier network will extend active power support to the disturbed one. And HVDC system no longer behaves as the

978-1-7281-6916-3/20/$31.00 ©2020 IEEE

2021 6th International Conference for Convergence in Technology (I2CT)
Pune, India. Apr 02-04, 2021

An Adaptive Master-Slave Technique using Converter Current Modulation in VSC-based MTDC System

Radheshyam Saha
Department of Electrical Engineering,
Delhi Technological University.
New Delhi, India
rshahacno@yahoo.com

Madhusudan Singh
Department of Electrical Engineering,
Delhi Technological University
New Delhi, India

Ashima Taneja
Department of Electrical Engineering,
Delhi Technological University
New Delhi, India
tanejaashima.1988@gmail.com

2021 6th International Conference for Convergence in Technology (I2CT) | 978-1-7281-8876-8/21/$31.00 ©2021 IEEE | DOI: 10.1109/I2CT51068.2021.9418191

Abstract—**The VSC-based multi terminal HVDC technology is gaining popularity in power system to integrate and efficiently operate multi-area AC systems of same or asynchronous frequency as one grid. Nevertheless, this technology has enabled to enhance controllability and stability of AC-DC integrated system. Depending upon the amount of power transfer between AC and DC systems, control strategy adopted for MTDC system varies. Master-Slave, Voltage Margin and Voltage Droop control are classical DC voltage control strategies for VSC-based MTDC systems. Although Voltage Droop technique is reliable but it suffers from drawbacks like inability to deliver constant active power to critical AC systems, inability to maintain DC voltage to a constant value, risk of irreversible switching from droop control mode to constant power control mode, etc. Voltage Margin technique is reliable than Master Slave control but suffers from power oscillations and large DC voltage overshoot when DC voltage control is transferred from main master controller to reserve controller. In this paper, an adaptive Master-Slave control technique with modulation of converter currents in Master terminal is proposed where direct-axis converter current is allowed to increase well up to maximum IGBT current carrying ability limit. Thus, augmented Master control scheme is able to compensate for more unbalanced power in DC grid than the conventional one thereby preventing severe DC overvoltage or arresting DC voltage from running down. The proposed control has enabled to improve the reliability and stability of AC-DC grid and is found to be more flexible than conventional Master-Slave control.**

Keywords—Vector control, Voltage source converters, Multiterminal DC systems, Master-slave control.

I. INTRODUCTION

The extensive use of HVDC transmission technologies is well justified because of many benefits offered by the DC transmission over AC transmission like unconstrained bulk power transmission over long distance, reduced power losses, flexible power flow control, effective conductor utilization, reduced RoWs, enhanced AC-DC power system stability, evacuation of power from remotely located RESs, islanding operation and many more [1,2]. Also, with advent of HVDC technology, it has been possible to not only interconnect two asynchronous systems stably but also an AC area can be divided into a multi-area system. The Voltage Source Converter (VSC) based HVDC technologies and topologies have ushered a new dimension to enhance the stability and security of the power system of large AC-DC network integration. Besides the various benefits indicated, few other attributes of these technologies are rapid power reversal, feasible multi-terminal systems, improved power quality, decoupled power flow control and dynamic reactive power compensation, etc. [3].

As regards the anatomy of the various control techniques that are employed in HVDC system, the vector current control scheme is used for control of VSC-based HVDC transmission in which generation of direct-axis reference current is done either by DC voltage control or by constant active power control. Similarly, generation of quadrature-axis reference current is done either by AC voltage control or by constant reactive power control. In a point to point VSC-HVDC system, one converter exercises DC voltage control while other is transferring constant active power [2].

Multi-terminal (MTDC) systems are formed by interconnecting DC grids of various converter terminals to a common DC voltage [1]. It is necessary to have proper DC voltage control and active power control [4]. At least one converter in MTDC grid is responsible for regulation of DC voltage so that balanced power exchange takes place in between AC and DC system [5]. Basically, MTDC control system is based upon how the generation of direct-axis reference current is done. Master-Slave (MS) control, Voltage Margin (VM) control and Voltage Droop (VD) control are three basic control techniques for VSC-MTDC systems whose features are depicted in Table I [1-3].

MS control is not so reliable due to its dependency on single converter for critical task of DC voltage regulation. Also, in case of increase in unbalanced power in DC grid, Master may lose its capability of maintaining stable DC voltage. As a result, overvoltage or undervoltage can occur due to lack of further DC voltage regulation [1,3]. For larger Voltage Margin controlled MTDC systems, more reserve masters are required, thus, making it cumbersome to define reference DC voltages for each converter station [1, 3-5]. In certain critical AC systems and in passive AC networks, it is desired to have a constant active power output from VSCs [3]. But voltage source converter stations controlled by VD technique are unable to deliver constant active power, if required [4]. With power losses & deviation in DC voltage neglected, this control cannot provide desired power flow without deviation from allotted power references [1]. In fact, such system is unable to regulate DC voltage to a fixed value rather only keeps the DC voltage within a permissible range [4]. Also, while transferring unbalanced power in grid, it does not take care of power margin left with the converter. Therefore, converter control may switch from droop control to constant power control mode which cannot be reversed [3]. Unlike droop controlled MTDC systems, DC voltage

2021 6th International Conference for Convergence in Technology (I2CT)
Pune, India. Apr 02-04, 2021

Two-Stage Stochastic Programming Model for Optimal Scheduling of RES-Based Virtual Power Plants in Electricity Markets

Meegada Indeevar Reddy
Department of Electrical Engineering, Delhi Technological University
Delhi, India
Indeevarreddy_mt2k19@dtu.ac.in

Radheshyam Saha
Department of Electrical Engineering, Delhi Technological University
Delhi, India
rshahacno@yahoo.com

Sudarshan K. Valluru
Department of Electrical Engineering, Delhi Technological University
Delhi, India
sudarshan_valluru@dce.ac.in

***Abstract*— To promote investment in the electricity sector, the deregulated electricity market regime has created an enabling environment to accelerate the all-around development of power generation, transmission and distribution systems. RE-based power generation is proliferating in the power sectors worldwide. Participation of large numbers of market players, and massive penetration of RE-generation have created enough complexities and has made fundamental changes in the deregulated electricity market conditions. Small scale RE generating units have limited participation in the electricity markets due to the uncertainties. These units integrate with other fossil fuel plants and forms as Virtual Power Plants (VPPs). Increasing participation of RE based VPPs in the competitive electricity market, has brought out further complexity in market operation primarily in terms of its generation scheduling, economic profitability, etc. In this paper a two-stage stochastic programming approach for optimal scheduling of VPPs in the electricity markets is presented, along with modeling of uncertainties in the electricity market price, available level of stochastic renewable generation and the request for reverse deployment. These uncertainties are modeled using scenario bounds and are formulated using stochastic programming approach. Simulation results are carried out on 4-h planning horizon.**

Keywords—*Electricity markets, Renewable Energy Sources (RES), Virtual Power Plants, Stochastic programming, Day Ahead Markets (DAM).*

I. INTRODUCTION

Power system utilities in the world are disintegrated and restructured, resulting in the diminishing of monopoly existed in the erstwhile vertically integrated markets. To promote investment in the power sector, deregulated market regime has created an enabling environment to accelerate development in generation, transmission and distribution systems. These result in large participation of market players, stakeholders, independent power producers, electricity traders, and pro-active roles of regulators. Massive penetration of renewable energy-based electricity generation is proliferating in every country around the world. It has made fundamental changes in the deregulated electricity market conditions. These changes affect the financial health of incumbent fossil fuel generators having inherently high marginal costs of generation per unit.

As per rough estimates, burning of widely used fuels like coal, bio-fuels pollute air over fifty times more carbon per unit of energy than wind, water, or solar power. Due to environmental conservation and increasing efforts to reduce global greenhouse gas emissions, efforts are being made for continuous policy reforms in the power sectors are on the cards across the globe, and thrusts are given towards sustainable sources of RE generation, replacing the pre-dominant nonrenewable electricity generations. Such transition is widely prevalent in U.S and European Union, which have set the milestone of electricity requirement with 100 percent renewable energy in near future [10-12].

Virtual power plants are integrated with several type of energy resources to aggregate total energy production from distributed energy resources (DERs) such as small hydro plants, roof top solar system, wind farms etc. VPP includes from small scale to medium scale renewable generating units, flexible loads, diesel generation sets etc. These utilities can from into a cluster of energy sources along with other fossil fuel power generating units. Increasing participation of VPPs which aim at an integrated approach of a cluster of small distributed RE based generating entities, and participating in the competitive electricity market as a single entity, has brought out further complexity in market operation primarily in terms of its generation scheduling, economic profitability, etc. VPP acts as an intermediary between distributed energy resources and the whole sale electricity markets and trade energy on behalf of DERs owners who themselves are unable to participate in that market. The concept of VPPs allows small scale RE generating units to get in to electricity markets.

The real time load demand is dynamic and so the power generation for balancing the load. Further, due to intermittency, and variability of RE sources and imperfect forecasting, there is randomness in RE generation (viz. wind farms, solar PV plants, etc), and it leads to the complexity of RE integration with the electricity grids. RE power being largely non-dispatchable, the generation scheduling of CPPs in combination with RE generators is a tough challenge being encountered by system operators in DAM and real time markets.

Understanding the uncertainties in the process of RE generation and are considered as stochastic process. To mitigate these uncertainties during the generation of RE sources, it is endeavored to integrate RE generating utilities with other generating units such as CPPs, storage units and flexible demands i.e., VPPs. In this paper, a two-stage stochastic programming is proposed to model these uncertainties present in the process of integrating these VPPs containing RE sources and finds an optimal solution for scheduling generating units in electricity market clearing process [4,7].

A brief overview of the present electricity market scenario is studied and market mechanisms coupled with

2021 6th International Conference for Convergence in Technology (I2CT) | 978-1-7281-8876-8/21/$31.00 ©2021 IEEE | DOI: 10.1109/I2CT51068.2021.9417927

bidding-based buy and sell of electricity in DAM and real time markets are well explained in [1-16]. The market clearing process in the electricity markets under various uncertainties is designed in [1]. The zonal market model with renewable integration is presented in [2] [3], [4]. Bidding strategy of virtual power plants (VPPs) for participating in energy and reserve markets is investigated in [5]. Introduction to the mathematical stochastic programming applied to electrical engineering is presented in [6]. Risk assessment in electricity markets and reserve market under uncertainties is carried out in [7]. Network constrained robust unit commitment model is explained in [8]. L. Tianqi et.al [9] analysed optimal scheduling of VPPs considering cost of battery loss. The statistical scenario of RE is illustrated in [10-13]. Impacts on power markets due to RE generation adequacy are presented in [14]. The challenges being faced by the electricity markets with the intermittence RE sources is explained in [15,16]. Optimal bidding based on Nash equilibrium strategy for VPP participation in the energy markets is proposed in [17]. However, the proposed approach adds to the existing research on RE based VPPs electricity markets.

This paper is organized into five sections. Section-1 provides RE-based market operation and pro-active role of Virtual power plants as introduction. Section-2 presents the impacts of renewable generation in deregulated markets. Stochastic programming methodology, modelling uncertainties and problem formulation for optimal scheduling process in electricity markets is explained in Section-3. Simulation results are illustrated in section-4 and section-5 ends with the conclusion followed by references.

II. Impact of RE generating units on deregulated Electricity Markets

RE generation has made fundamental changes in the market conditions. Historically, there are steep reductions in costs of RES generation over the time and per unit cost is economical and compared to the cost of fossil fuel-based generation. RE penetration into the markets has resulted in reduction of wholesale electricity prices. It is indicated in [13], the levelized cost of electricity (LCOE) between 2009-2017 for PVs fell from $304 per MWh to just $86, a reduction of 72%. Onshore wind's LCOE dropped from $93 to $67 per MWh, a reduction of 27%. These factors and the feature of insignificant greenhouse gas emissions are instrumental to make a paradigm shift to create market of renewable. However, it has created a large impact on the economic profitability of conventional generators and considerably affects the financial health of the stakeholders of fossil fuel generators. It has also transpired that massive penetration of RE is and will be leading to even negative electricity prices, i.e., conventional generators are required to pay to produce electricity [3].

Uncertainty of RE generation is another critical factor which affects the scheduling and operation of the grid [15]. VPPs enable to provide a possible solution to mitigate such issues with its group of generating units (both conventional and RE sources), storage units, biomass plants and flexible demands. These VPPs can optimize their energy sources utilizing conventional plants during its low RE production and participate in the markets during its high RE production through storage units. It also reveals the importance of conventional sources in supporting the system. These traditional generators can act as capacity plants in the capacity markets.

In the context of economic profitability of stakeholders [10-13], optimal utilization of resources to meet end user requirements, and for mitigating imbalance of load-generation dynamics in RE dominated electricity market, stochastic and optimal scheduling of VPPs is made as a part of market research.

III. Stochastic Optimal scheduling Program

This section analyses the optimal scheduling problem of the electricity markets where virtual power plants (VPP) sells or buys the energy with the objective of profit maximization. On other hand, reserve markets provide the flexibility to increase or decrease the total energy production of VPPs upon the request of the system operator.

The Day-Ahead and reserve electricity markets are considered in this section to analyse the market scheduling decisions one day in advance. While making this scheduling decision the VPPs faces a number of uncertainties [1,9]. Following are the uncertainties faced in the market scheduling process:

- The market prices include the day-ahead market prices and the reserve markets prices (for both capacity and energy).
- Stochastic nature of the available renewable generating unit's production level.
- The requests to deploy reserves sources by the system operator.

The proposed uncertainties are modeled for obtaining optimal market scheduling decisions. As the proposed approach is probabilistic and not deterministic in nature, inappropriate modeling will result in loss or profit to the VPPs and even results in an infeasible operation of utilities/ generation and demand assets [18].

TABLE I. Nomenclature

Notation	Definition
Ω^C	Set of Conventional Power Plants
Ω^D	Set of Demands
Ω^R	set of renewable energy generating units
Ω^S	Set of storage units
Ω^T	Scheduling Time periods
Ω^ϑ	Set of discrete scenarios
$C_C^{C,F}$	Online cost of conventional generating unit c [$/h]
$C_C^{C,V}$	Variable cost of conventional generating unit c [$/h]
P_{ct}^C	Power generation of the conventional power plants in time period *t* [MW]
P_{dt}^D	demand *d* power consumption level in the time period *t* [MW]
P_{rt}^R	RE generating unit *r* production level during the time period *t*
$P_{rt}^{R,A}$	Available RE generating limit of unit *r* in the time period *t*
$P_{st}^{S,D}$	Power discharging level of storage unit *s* in the time period *t*
$P_{st}^{S,C}$	Charging level of storage unit *s* in the time period *t* [MW]
e_{st}^s	Energy stored by the storage unit *s* in the time period *t* [MWh]
P_t^{R+}	Power capacity traded in up-reserve market in time period *t*
P_t^{R-}	Power capacity traded in down-reserve market in time period *t*
P_t^E	Amount of Power traded in the market during the time period *t*

A. Modelling Uncertainties

The uncertainties mentioned above are modelled using a set of predefined discrete scenario realizations indicated by $\vartheta \epsilon \emptyset^V$. Each scenario of ϑ is defined by the parameters $\mu_{\vartheta t}^E, \tilde{\mu}_{\vartheta t}^{R+}, \mu_{\vartheta t}^{R+}, \tilde{\mu}_{\vartheta t}^{R-}, \mu_{\vartheta t}^{R-}, K_{\vartheta t}^{R-}, K_{\vartheta t}^{R-}$, and $P_{rt\vartheta}^{R,A}$ that indicates energy market price, market price acquired for power capacity in the down-reverse market, the up and down-reverse deployment request, and the available generating levels of stochastic RE generating units respectively. Each scenario ϑ is defined with probability of occurrence π_ϑ. The sum of overall probabilities of the scenarios is equal to 1, i.e., $\sum_{\vartheta \epsilon \emptyset^V} \pi_\vartheta = 1$.

B. Problem Formulation

The optimal decision-making problem under these scenarios is modelled as a two-stage stochastic programming model and is interpreted as follows:

$$max_{\varphi^V} \sum_{\vartheta \epsilon \emptyset^v} \Pi_\vartheta \left\{ \sum_{t \in \Omega^T} \left((\mu_t^E P_t^E \Delta t) + (\tilde{\mu}_{\vartheta t}^{R+} + K_{\vartheta t}^{R+} \mu_{\vartheta t}^{R+} \Delta t) P_t^{R+} + (\tilde{\mu}_{\vartheta t}^{R-} - K_{\vartheta t}^{R-} \mu_{\vartheta t}^{R-} \Delta t) P_t^{R-} - \sum_{C \in \Omega^C} \left(C_C^{C,F} u_{ct}^C + C_C^{C,V} P_{ct\vartheta}^C \Delta t \right) \right) \right\} \quad (1)$$

Subject to: (2)

$$\underline{P}_t^E \le P_t^E \le \overline{P}_t^E$$

$$\underline{P}_t^{R+} \le P_t^{R+} \le \overline{P}_t^{R+} \quad (3)$$

$$\underline{P}_t^{R-} \le P_t^{R-} \le \overline{P}_t^{R-} \quad (4)$$

$$P_t^E + K_{\vartheta t}^{R+} P_t^{R+} - K_{\vartheta t}^{R-} P_t^{R-} = \sum_{C \in \Omega^C} P_{ct\vartheta}^C + + \sum_{r \in \Omega^R} P_{rt\vartheta}^R + \sum_{s \in \Omega^S} \left(P_{st\vartheta}^{S,D} - P_{st\vartheta}^{S,C} \right) - \sum_{d \epsilon \Omega^D} P_{dt\vartheta}^D \quad (5)$$

$$\underline{P}_{dt}^D \le P_{dt\vartheta}^D \le \overline{P}_{dt}^D \quad ; \forall d \in \Omega^D \quad (6)$$

$$\sum_{t \in \Omega^T} P_{dt\vartheta}^D \Delta t \ge \underline{E}_d^D \quad ; \forall d \in \Omega^D \quad (7)$$

$$\underline{P}_{ct}^C u_{ct}^C \le P_{ct\vartheta}^C \le \overline{P}_{dt}^C u_{ct}^C \quad ; \forall C \in \Omega^C \quad (8)$$

$$0 \le P_{rt\vartheta}^R \le P_{rt\vartheta}^{R,A} \quad ; \forall R \in \Omega^R \quad (9)$$

$$\underline{P}_{st}^{S,C} \le P_{st\vartheta}^{S,C} \le \overline{P}_{st}^{S,C} \quad ; \forall S \in \Omega^S \quad (10)$$

$$\underline{P}_{st}^{S,D} \le P_{st\vartheta}^{S,D} \le \overline{P}_{st}^{S,D} \quad ; \forall S \in \Omega^S \quad (11)$$

$$e_{st\vartheta}^s = e_{s(t-1)\vartheta}^S + P_{st\vartheta}^{S,C} \Delta t \eta_s^{S,C} - \frac{P_{st\vartheta}^{S,D} \Delta t}{\eta_s^{S,D}} \quad ; \forall S \in \Omega^S \quad (12)$$

$$\underline{E}_{st}^S \le e_{st\vartheta}^S \le \overline{E}_{st}^S \quad ; \forall S \in \Omega^S \quad (13)$$

Where set $\varphi^V = \left\{ P_t^E, P_t^{R+}, P_t^{R-}, \forall t \in \Omega^T; u_{ct}^C, \forall C \in \Omega^C; P_{ct\vartheta}^C, \forall C \in \Omega^C; P_{rt\vartheta}^R, \forall R \in \Omega^R; P_{st\vartheta}^{S,C}, ; \forall S \in \Omega^S; P_{st\vartheta}^{S,D}, \forall S \in \Omega^S; e_{st\vartheta}^s, ; \forall S \in \Omega^S \right\} \forall t \in \Omega^T, \forall \vartheta \epsilon \emptyset^V$ are the optimization variables in the above problem. Π_ϑ indicates, weight of each scenario ϑ [7,8,9]. VPPs objective is described by the Eq. (1) throughout the planning horizon and consists of the following terms:

- The term $\mu_t^E P_t^E \Delta t, \forall t \in \Omega^T$ represents the revenues acquired by the VPPs for their participation in the DA markets. Here the variable P_t^E may be +ve (if VPPs sell power in the DA market) and -ve (if the VPPs buy power in the DA markets).
- The term $(\tilde{\mu}_{\vartheta t}^{R+} + K_{\vartheta t}^{R+} \mu_{\vartheta t}^{R+} \Delta t) P_t^{R+}, \forall t \in \Omega^T$ represents the revenue obtained by the VPP for participating in the Up-reserve markets. These revenues are again divided into $(\tilde{\mu}_{\vartheta t}^{R+} P_t^{R+})$ capacity payments and $(K_{\vartheta t}^{R+} \mu_{\vartheta t}^{R+} \Delta t P_t^{R+})$ energy payments.
- The term $(\tilde{\mu}_{\vartheta t}^{R-} - K_{\vartheta t}^{R-} \mu_{\vartheta t}^{R-} \Delta t) P_t^{R-}, \forall t \in \Omega^T$ represents the revenue obtained by the VPP for participating in the Down-reserve markets. These revenues are again classified into $(\tilde{\mu}_{\vartheta t}^{R-} P_t^{R-})$ capacity payments and $(K_{\vartheta t}^{R-} \mu_{\vartheta t}^{R-} \Delta t P_t^{R-})$ energy payments.
- Variable cost incurred by the CPPs is represented by the term $(C_C^{C,F} u_{ct}^C + C_C^{C,F} P_{ct\vartheta}^C \Delta t); \forall C \in \Omega^C, \forall t \in \Omega^T$

Where Eqs. (2), (3) and (4) are the constraints, representing upper and lower bounds on the amount of power traded in the DA, up, and down-reserve markets respectively. Eq. (5) represents the power balancing constraint. Eqs. (6) and (7) puts power consumption limits on the demands. $u_{ct}^C \in \{0,1\}; \forall C \in \Omega^C, \forall t \in \Omega^T$ denotes binary variable, it represents the on/off status of CPP. Constraints in the Eqs. (8), and (9) limits the power produced by the CPPs and stochastic RE generation level respectively. Eqs. (9) and (10) represents the constraints on the charging and discharging level of storage units, while the Eq. (12) represents the energy production level in storage units and Eq. (13) represents the limiting constraint on the energy level of the storage units. The above problem is a Mixed Integer Linear Programming (MILP) problem solved using CLPEX solver.

IV. Simulation Results

The proposed two-stage stochastic model for optimal scheduling is tested on 4-hour planning horizon, and the required data is collected from [18]. The simulation results are implemented in GAMS software using CLPEX solver on a PC with an Intel i7 3.6GHZ CPU and 8-GB RAM.

The maximum power traded (sold/buy) in the energy market is limited to 100MW. The up and down reverse market capacity is limited at 50 MW. Energy Market prices along with up and down reverse market prices for the power capacity are presented in Table-2. Generation limits of the CPPs and their economic data along with the flexible demand data is referred from IEEE-5 bus system. The forecasted wind power production level is provided in Table-3. Reverse deployment request is considered to be 80% of the power capacity scheduled in down reserve market during the time period-2, similarly for up reserve market 50% and 100% of scheduling capacity are requested during the time period-1 and 3 respectively. No reserve deployment is requested during the time period-4. This data is assumed and considered based on the system operators request for the reverse deployments.

In the above two-stage stochastic programming model, the uncertainty in the RE (wind) generating levels along with the uncertainty present in the reserve deployment request are modeled by using two equiprobable scenarios in each stage. Thus 4 scenarios (two of each) are considered. For the sake of simplicity these scenarios are independent of each other.

TABLE II. ENERGY AND REVERSE MARKETS PRICE DATA

Time Period	Price [$/MWh]				
	Energy Markets	*Up reserve market*		*Down reserve market*	
		Energy	*Capacity*	*Energy*	*Capacity*
1	12	14	4	14	4
2	14	15	10	38	10
3	22	30	8	26	8
4	32	20	6	25	6

TABLE III. TOATAL WIND FORECASTING LEVEL FOR DIFFERENT TIME PERIODS AND WEIGHTS[PU]

Time Period	Wind Power Generating level [MW]			Scenario Weights
	R_1	R_2	R_3	
1	70	100	120	0.25
2	100	83	140	0.25
3	95	75	115	0.25
4	55	80	100	0.25

The proposed model presented in the section-III is runed by the system operator to determine optimal scheduling for each generating unit in each time period. Considering the data presented in the tables-II and III, the optimal power scheduled and market prices in Day-ahead and reserve markets are presented and explained in Figs. 1 to 7.

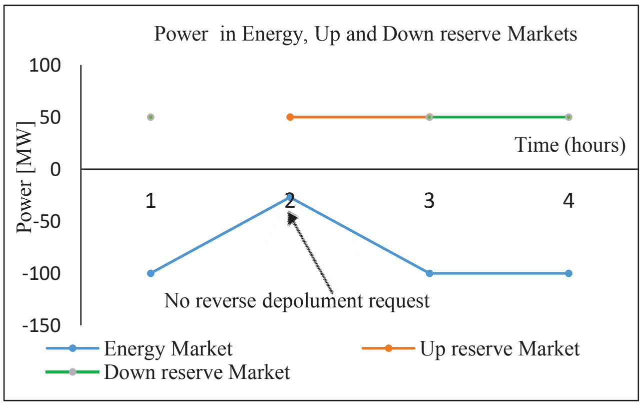

Fig. 1. Plants Power traded in energy, up-reserve and down reserve markets

VPPs participate in the energy markets and submit their bids based upon their demand levels in the specific time period, these bids are submitted in terms of price and quantity to the system operator. Fig. 1 shows, the optimal amount of power traded in each time period in the energy, up and down reserve markets. In these markets the VPPs decides to buy the energy, expect for the time period-2 when its demand level is being low and during this period energy is supplied by their own renewable generating units. In all other cases the VPPs tries to buy the energy in the energy market. In the case of up reserve market, the power is traded in time periods 2 and 3. While in the case of down reserve market power is traded during the periods 1, 3 and 4. No power is traded during the time period-2. This is because of the maximum demand levels and low prices for the reserve deployment as explained in Table-II.

Based up on the amount of power traded in the energy and reserve markets, conventional power plants are scheduled. During the low demand level i.e., during the time period-2, these plants are turned off. Fig. 2 shows, scheduling of CPP. The power plants with highest economical prices are not scheduled for the entire market operation as shown in Fig 5. The renewable generation is maximum at each time period as shown in the Fig. 4. Power consumption levels in each time period is same expect for the time period T-2. In order to supply their demand level during the maximum demand periods, VPPs enter in to the power markets. Therefore, based on the market prices the VPP decides to buy maximum power from RE sources in the markets.

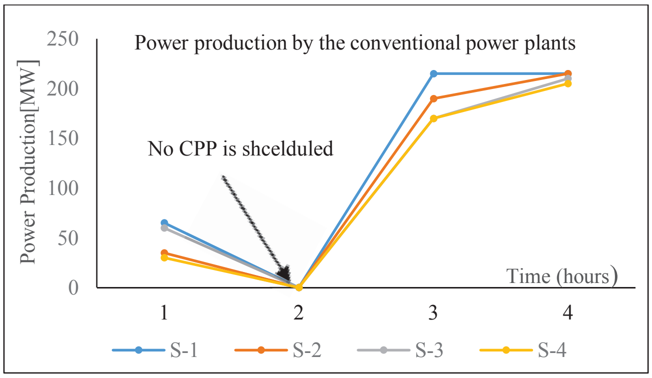

Fig. 2. Power consumption by the conventional power planys in the market

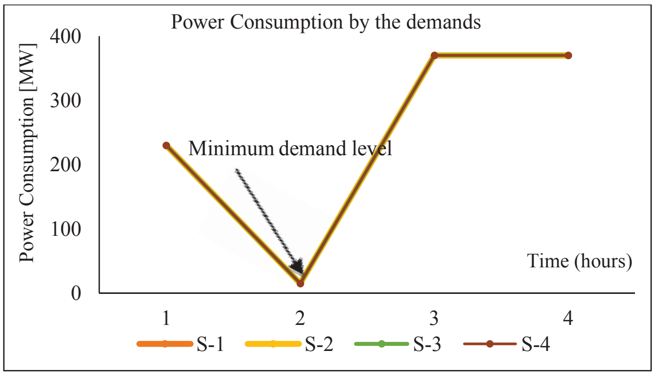

Fig. 3. Power consumption by the demand in the market

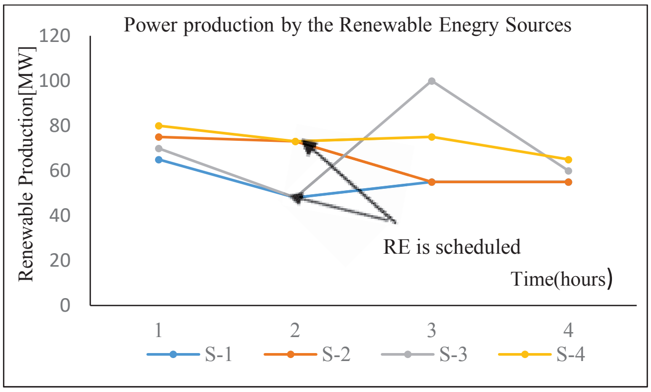

Fig. 4. Forecasting Power generating level of Wind power source

From the above optimal scheduling process, it is clear, that the stochastic RE sources are made to dispatch in all time periods and based on the power demand level and market prices the system operator request for up and down reverse deployments during a sepefic time period.

The conventional power plants are scheduled only when the required demand is more than the RE and reverse deployment capacity. Fig.5 shows scheduled dispatch of CPPs. During every hour generator (G-4) is not dispatched. Similarly, during second period no CPP is scheduled. This puts economic burden on the conventional generators. The prices incurred during the power production is less than the revenues obtained. Hence, it is required to provide policy incentives and to take standard tariff policy mechanism for conventional generation. Updating to the current technology, increasing ramp up and ramp down rates of the generators may make their way possible to compete with the RE sources.

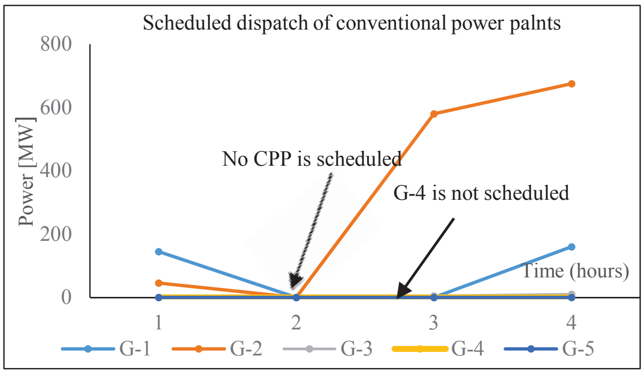

Fig. 5.Scheduled power dispatch of conventional power plants

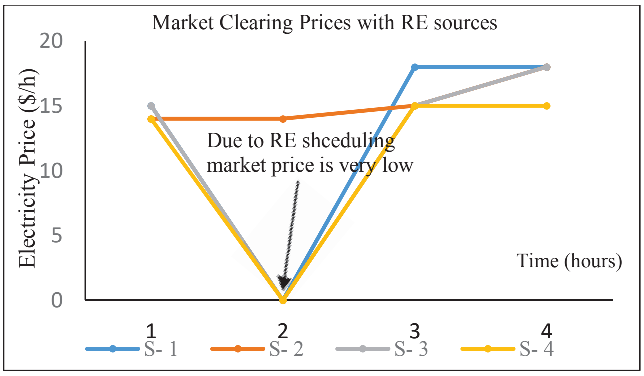

Fig. 6.Market clearing prices in $/h with RE sources for different time periods.

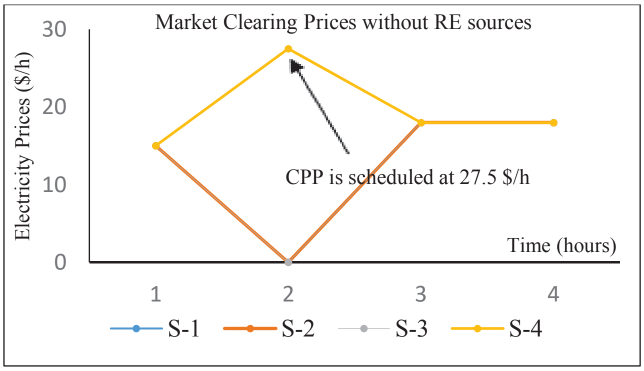

Fig. 7.Market clearing prices in $/h without RE sources for different time periods.

Fig.6 and Fig.7 represents market clearing price ($/h) variations with and without RE sources. It is observed that MCP's without RE sources is always greater than the MCP'S with RE. Therefore, it is clear that the conventional generators are forced to generate power for lesser prices. This price variations will result in economic losses. Therefore, it is required to provide cost-based policy incentives for the conventional plants. Some of the countries are following fed in tariff policy, purchase obligations and contract for difference mechanism to create a balance pricing mechanism.

The above simulation result has established that during low demand periods VPPs optimizes its resources by using RE (wind) generation only. During maximum demand periods CPPs are scheduled, and reserve deployment requests are made accordingly to the system operator request. With interest participation of VPPs market price levied on the consumers is reduced but burden on the conventional generators increases. The simulation graphs shown in Fig.6 and 7 has clearly indicated the price variations with and without RE sources. This clearly indicate that the VPPs in the electricity market are acting as price makers and sometimes as price takers.

The above two stage stochastic problem is executed using deterministic approach, in such case the optimal scheduling of VPP is found infeasible. This is due to the error while providing reverse deployment request. This highlights the importance of an accurate modelling of the uncertainties in the problem. Economic impact on CPPs due to RE sources can also be interpretated from the above results.

V. CONCULSION

Power and energy balancing mechanisms are evolutionary in market operation from the cost economics angle. It depends on RE policies, power sector reform strategies, price discovery mechanisms, generation scheduling economics, load management techniques, role of VPPs, etc. Like every generator looking for its profitability and services to the system operation. VPPs with its resources look for maximization of their profits. The proposed two-stage stochastic modelling for optimal scheduling of VPPs in electricity markets has established the merits of its generation scheduling to mitigate certain uncertainties as explained in Para-A, section-III of this paper. The simulation work provides impressive results for accurate optimal scheduling of the generating units of VPPs. This method may be extended to large scale market operations and big power system networks by dividing the system into several subsystems. In future, the presented method may be extended to model forecasting uncertainties along with modelling of large solar generating units.

REFERENCES

[1] Conejo, A.J., Carrión, M., Morales, J.M.: Decision Making Under Uncertainty in Electricity Markets. Springer, New York, US (2010).

[2] I. Aravena and A. Papavasiliou, "Renewable Energy Integration in Zonal Markets," *IEEE Trans on Power Systems*, vol. 32, no. 2, pp. 1334–1349, 2017.

[3] R.Bayindir, S.Demirbas, E.Irmak, et al., "Effects of renewable energy sources on the power system", 2016 IEEE conference (PEMC), pp.1-6, Sep-2016.

[4] B. Jie,et.al, "An analysis of market mechanism and bidding strategy for power balancing market mixed by conventional and RE,"

International Conf on the European Energy Market, EEM, 2017, pp.1–6.

[5] Mashhour, E., Moghaddas-Tafreshi, S.M.: Bidding strategy of virtual power plant for participating in energy and spinning reserve markets–Part-I: *Problem form IEEE Trans*. Power Syst. 26(2), 949–956 (2011).

[6] Birge, J.R, Louveaux.F, “Introduction to Stochastic Programming”, 2nd edn. *Springer*, New York, US (2011)

[7] S. R. Dabbagh and M. K. Sheikh-El-Eslami, "Risk Assessment of Virtual Power Plants Offering in Energy and Reserve Markets," in *IEEE Transactions on Power Systems*, vol. 31, no. 5, pp. 3572-3582, Sept. 2016, doi: 10.1109/TPWRS.2015.2493182.

[8] Jiang.T, Zhang.M, Li.G, Guan Y “Two stage network constrained robust unit comitment problem”, *Eur J oper Res* 234(3),751-7-7

[9] L. Tianqi et al., "Analysis of Optimal Scheduling Model for Virtual Power Plants Considering the Cost of Battery Loss," 2019 *2nd International Conference on Information Systems and Computer Aided Education (ICISCAE), Dalian, China*, 2019, pp. 218-222, doi: 10.1109/ICISCAE48440.2019.221621.

[10] D. Spencer, “B.P. Statistical Review of World Energy Statistical Review of World,” *The Editor B.P. Statistical Review of World Energy*, pp. 1–69, 2019.

[11] IEA, “Market Report Series: Renewables 2019 Analysis and Forecasts to 2024,” 2019.

[12] World Bank, “The World Bank: state and trends of the carbon market,” 2010.

[13] Renewable Energy Agency International IRENA, “Renewable Energy Market Analysis: Latin America,” 2019.

[14] Stefan Jaehnert and Gerard Doorman, “Analyzing the generation adequacy in power markets with renewable energy sources”, 11th *International Conference on the European Energy Market*, pp.1-6, 2014.

[15] P. L. Joskow, “Challenges for Wholesale Generation at Scale: Intermittent Renewable Electricity Markets with The U.S. Experience,” 2009

[16] Morales J.M, Conejo A.J, Madsen. H, Pinson.P, Zungo.M, “Integrating Renewables in ELecrcity Markets-Operational Issues”, *springer*, New york, USA, 2014

[17] H. Nezamabadi, P. Nezamabadi, M. Setayeshnazar and G. B. Gharehpetian, "Participation of virtual power plants in energy market with optimal bidding based on Nash-SFE Equilibrium Strategy and considering interruptible load," *The 3rd Conference on Thermal Power Plants*, Tehran, 2011, pp. 1-6.

[18] Luis Baringo and, Morteza Rahimiyan, “Virtual Power Plants and Electrcity Markets”, e-Book, *Springer Nature Switzerland AG 2020,* https://doi.org/10.1007/978-3-030-47602-1

Modelling Financially Motivated Cyber Attacks on Electricity Markets Using Mixed Integer Linear Programming

Meegada Indeevar Reddy, Radheshyam Saha, and Sudharshan K. Valluru
Department of Electrical Engineering,Delhi Technological Univesity.

***Abstract*— With the vast expansion of grid network and enhancement of Communication system, Cyber security reinforcement is of paramount importance for reliable and secure power system operation. Cyber-attacks on electricity markets acquire financial profits to the adversary. In this paper a modest attempt is made to model the cyber attacker's objective of profit maximization by injecting false data into Day-ahead and Real Time electricity markets. It is considered that attacker runs a bi-level optimization problem which includes attacker's profit maximization objective and market clearing problem for finding out the optimal attack measurements. While manipulating the measuring devices like RTUs, the attacker takes care to avoid being detected by the bad data detection (BDD) procedure run by the ISO. This paper focuses on financially motivated FDI attacks considering attacker as one of the virtual players in electricity market. A novel attacking model is designed using bi-level optimization problem where attacker aims to gain financial benefits by misleading market clearing problem. Potential impact of financially motivated False Data Injection (FDI) attacks on electricity markets is presented by considering PJM 5-bus system. The simulation results show the sharp impact on Locational Marginal Prices (LMPs) in fulfilling the attacker's objective, and the distinct relationship between LMPs and the market clearing prices during the attack.**

Keywords*— *Cyber Attacks, Day-Ahead Market (DAM), Real Time Market (RTM), Mixed Integer Linear Programming (MILP), optimization, Locational Marginal Prices (LMPs), Congestion.

I. Introduction

Power system is a strongly interconnected electricity network coupled with state-of-the-art communication network for transmitting and distributing electricity from generating stations to load centers. This huge network is consistently controlled, operated, and monitored in real-time mode by IT-enabled SCADA system from control centers by ISO/TSO. All the real-time operational data of the power system are picked-up through remote terminal units (RTUs), transducers, and various sensing devices. This data is transmitted and processed by SCADA at the control centers to enable system operators to efficiently control and handle the grid dynamics in the competitive power markets. With the continuous expansion of the electricity grid, the risk of cyber-attacks to the real-time system has become a serious issue Although the SCADA System has firewall as the first stage of security to the communication network, still cyber-threat is a challenging phenomenon for ISO to defend its integrity.

At present, the power sector is operating as day-ahead (DA) and real-time (RT) markets. In these markets, various market players including sellers, buyers, and traders participate through an online platform of Power Exchanges and submit their bids in quantity and price. The DC-OPF model is used to determine LMPs, considering the topology and physical constraints of the power system and power demand as per the load forecasting values, and there are mismatches from the actual demand values during the real-time market operation. Hence there is an accuracy problem in the power system state estimation. Adversary takes this as a chance and manipulates the meter readings by injecting false data. Meanwhile, the attacker takes care of not being detected in the BDD procedure.

The paper is organized into six sections. Section-I covers the cyber-attack strategy with its introduction. In section-II, the market-clearing problem of both DA and RT markets using SCED is presented. Section-III discusses the power system state estimation and optimal attacking problem. In section IV, the implicit relationship between the upper and lower level problem is presented along with converting bi-level attacking problem into single-level MILP problem. section V discusses simulation results on PJM-5bus System with and without attack. Section VI ends with the conclusion.

A. Current state of Art

As a matter of fact, cyber-attacks on power systems are generally classified into two types. The first type of attacks aims in creating damage to the grid and the latter type focus on financial gains. FDI was first studied by Liu et al. [1].

In the foremost type, adversary estimates attack vulnerability areas to inject false data into the measuring devices, which leads to grid failure or shutdown of some major grid components. These attacks are investigated in [2-5] by using various methods. Stealthy FDI detection using machine learning is studied in [3]. AGC detection is a popular technique presented in [4]. Statistical structure learning to ensure data integrity in smart grid is examined in [5]. FDI modelling and counter measures are discussed in [6]. Power grid resilience against FDIA is demonstrated in [7]. A survey on FDIAs is presented in [8]. Forecasting aided imperfected attack against state estimation is presented in [9].

The second type of attack is based on gaining financial benefits. In [10] a special class of FDI attacks using load distribution has been investigated. Attacks by overloading the transmission lines by introducing corrupt generators and load forecasting error in the Security Constrained Economic Dispatch is presented in [11-14] which results in LMP shift. Financially motivated attacks have been investigated in [15]. Modelling dummy data attack vector which is used to Change congestion pattern is presented in [16], A new framework in designing FDI attack using stochastic robustness by limited adversary is presented in [19]. Deep learning techniques for FDI attack detection on smart grid is examined in [20]. A non-linear auto regressive exogenous configuration of ANN is used to identify FDI attack on state estimation is formulated in [21]. Market decision making, non-linear optimization problems in electricity markets, along with Bi-level optimization problems in power system is presented in [22,23,24].

II. Electricity Markets Operation

Deregulated electricity markets conduct electricity trading in competitive environment. Buyers and sellers submit their bids in terms of both quantity and prices. An independent system operator (ISO) is a third-party regulator, and independent of both supplier and consumer is responsible for determining market clearing price (LMPs) and managing transmission network. DC-lossless optimal power flow model along with LMP calculations for both the DA and RT markets are carried out as presented below with the nomenclature given in Table-I.

TABLE I. Nomenclature

Definitions	
Ω_g, Ω_d	Set of generators and demands respectively in the network
T	Operating time period
Ω_n	Set of generators and demand connected to bus n
S_{lj}	Generalized shift factor matrix
N_{bus}	Number of buses in the network
Ω_l	Number of branches (lines) in the network

A. Day-Ahead Market Operation

In the DA market, ISO performs optimal calculations to maximize Social welfare and to minimize aggregate cost of generation for given load dispatch. DA market allows submitting bids one day in advance and the dispatch is scheduled for the next following day. The optimization problem needs to satisfy the network topology and physical constraints of the network. The above DA market optimization objective is presented in [3,8,17] and which can be depicted as follows

$$\min_{\lambda, P_{it}, D_{jt}} R_{DA} = \sum_{i=1}^{\Omega_g}\sum_{t=1}^{T} C_{it}P_{it} - \sum_{j=1}^{\Omega_d}\sum_{t=1}^{T} B_{jt}D_{jt} \quad (1)$$

$$S.t \quad \sum_{i\in\Omega_n} P_{it} = \sum_{j\in\Omega_n} D_{jt} \qquad \forall\Omega_n \in N_{bus};\ (\lambda_t) \quad (2)$$

$$P_{it}^{min} \le P_{it} \le P_{it}^{max} \qquad (\mu_{it}^{max}, \mu_{it}^{min}) \quad (3)$$

$$D_{jt}^{min} \le D_{jt} \le D_{jt}^{max} \qquad (\gamma_{it}^{max}, \gamma_{it}^{min}) \quad (4)$$

$$F_{l}^{min} \le F_{lt} \le F_{l}^{max} \qquad \forall l \in \Omega_l;\ (\vartheta_{it}^{max}, \vartheta_{it}^{min}) \quad (5)$$

Where C_{it}, P_{it} and B_{jt}, D_{jt} are prices ($/MWh), quantity (MWh) offered by generators (suppliers) and demands (consumers) respectively. R_{DA} in Eq. (1) shows objective function of maximizing social welfare and minimizing cost of generation. Where $F_{lt} = \sum_{i=1}^{\Omega_n} S_{lj}\left(\sum_{i=1}^{\Omega_g} P_{it} - \sum_{j=1}^{\Omega_d} D_{jt}\right)$; $\forall n \in N_{bus}$ represents power flow in the transmission lines. Eq. (2) represents balancing constraints. Eq. (3), Eq. (4) and Eq. (5) puts upper and lower bounds for generating capacity, load demand and transmission line capacity respectively, and λ, μ_{it}^{max}, μ_{it}^{min}, γ_{it}^{max}, γ_{it}^{min}, ϑ_{it}^{max}, ϑ_{it}^{min} are corresponding dual variables of Eq. (2), Eq. (3), Eq. (4) and Eq. (5) respectively. Locational Marginal Prices in ($/h) at each bus in the DA market is interpreted as follows

$$LMP_{it}^{DA} = \lambda_t + \sum_{l\in\Omega_l} \vartheta_{lt}^{min} * S_{li} - \sum_{l\in\Omega_l} \vartheta_{lt}^{max} * S_{li} \quad (6)$$

B. Real Time Market operation

Based on the state estimation performed on the data collected from the different measuring units, the ISO aims to minimize the incremental change in the variables i.e., difference between the scheduled value and measured values in DA market. RT market is operated for every 5 minute and another LMP vector is calculated based on this run time data [8,17]. RT market clearing solves SCED optimization problem and is formulated as

$$\min_{\lambda, \Delta P_{it}, \Delta D_{jt}} R_{RT} = \sum_{i=1}^{\Omega_g}\sum_{t=1}^{T} C_{it}\Delta P_{it} - \sum_{j=1}^{\Omega_d}\sum_{t=1}^{T} B_{jt}\Delta D_{jt} \quad (7)$$

$$S.t \quad \sum_{i\in\Omega_n} \Delta P_{it} = \sum_{j\in\Omega_n} \Delta D_{jt} \qquad \forall\Omega_n \in N_{bus};\ (\tilde{\lambda}_t) \quad (8)$$

$$\Delta P_{it}^{min} \le \Delta P_{it} \le \Delta P_{it}^{max} \qquad (\tilde{\mu}_{it}^{max}, \tilde{\mu}_{it}^{min}) \quad (9)$$

$$\tau D_{jt}^{min} \le \Delta D_{jt} \le \tau D_{jt}^{max} \qquad (\tilde{\gamma}_{it}^{max}, \tilde{\gamma}_{it}^{min}) \quad (10)$$

$$\Delta F_{lt} \le 0 \qquad \forall l \in Cl_+;\ (\tilde{\vartheta}_{it}^{max}) \quad (11)$$

$$\Delta F_{lt} \ge 0 \qquad \forall l \in Cl_-;\ (\tilde{\vartheta}_{it}^{min}) \quad (12)$$

Where ΔP_{it},ΔD_{jt} represent the incremental change in power generation and load demand values, R_{RT} in Eq. (7) represents the ISO objective function of minimizing incremental cost of generation. In Eq. (9) and Eq. (10) upper and lower bounds are imposed on incremental power generation and demand values respectively. Where $\Delta F_{lt} = \sum_{i=1, l\in\Omega_l}^{\Omega_n} S_{lj}\left(\sum_{i=1}^{\Omega_g} \Delta P_{it} - \sum_{j=1}^{\Omega_d} \Delta D_{jt}\right)$ represents change in power flow. $\tilde{\lambda}_t$, $\tilde{\mu}_{it}^{max}$, $\tilde{\mu}_{it}^{min}$, $\tilde{\gamma}_{it}^{max}$, $\tilde{\gamma}_{it}^{min}$, $\tilde{\vartheta}_{it}^{max}$, $\tilde{\vartheta}_{it}^{min}$ are dual variables of Eq. (8), Eq. (9), Eq. (10), (11) and Eq. (12) respectively. Furthermore, ISO computes line flow changes through each transmission line *l* and tries to keep line flow measurements within the limits, (for both positively ($l \in Cl_+ : F_l \ge F_l^{max}$)and negatively congested lines($l \in Cl_- : F_l \le F_l^{min}$) [8,18]. LMPs in ($/h) at each bus in the RT market are governed by the following equation

$$LMP_{it}^{RT} = \tilde{\lambda}_t + \sum_{l\in Cl_-} \tilde{\vartheta}_{lt}^{min} * S_{li} - \sum_{l\in Cl_+} \tilde{\vartheta}_{lt}^{max} * S_{li} \quad (13)$$

From the above market clearing problem, if the attacker buys certain amount of power ($D_{it}\ MW$) at LMP_i^{RT} in DA market and after compromising the meter data, sells ($\Delta P_{it}\ MW$) in real time market at LMP_i^{RT}, its profit would be $[LMP_{it}^{RT} \times (\Delta P_{it}) - LMP_{it}^{DA} \times (D_{it})]$$/h. and the same follows, if the attacker sells electricity for expensive price in DA market and buys it for cheap price in real time market

[3,17]. The profit in (\$/h) that the attacker obtains by the above virtual electricity trading is given by

$$\text{profit} = \sum_{i=1}^{\Omega_n}\sum_{t=1}^{T}\left[LMP_{it}^{RT}\Delta P_{it} - LMP_{it}^{DA}D_{it}\right] + \left[LMP_{it}^{DA}P_{it} - LMP_{it}^{RT}\Delta D_{it}\right]$$
$$= \sum_{i=1}^{\Omega_n}\sum_{t=1}^{T}\left[LMP_{it}^{RT}(\Delta P_{it} - \Delta D_{it}) + LMP_{it}^{DA}(P_{it} - D_{it})\right] \quad (14)$$

III. Power System State Estimation

For a DC linearized lossless transmission system with $n+1$ buses and a set $M = \{1,2,3,\dots m\}$ of meters. The states are typically bus voltages and phase angle. The meter data (RTU's) typically includes real power injection, branch power flow in each transmission line. 'J' is the Jacobin matrix. The relationship between the meter data 'Z' and the system states X is

$$Z = JX + e \quad (15)$$

Where, e is the measurement error matrix and is considered to follow gaussian distribution with zero mean and co-variance matrix $R, J \in R^{m\times n}$. 'e' matrix represents the deviation of run time states from the scheduled optimal states. The state estimation problem is to find an estimate $\hat{X}$ of state variable X to the best suit of the meter measurements [13,18], and that minimizes weighted least square error is given by

$$\hat{X} = argmin\{(Z - JX)^T R(Z - JX)\} \quad (16)$$
$$\hat{X} = (J^T R^{-1} H)^{-1} J^T R^{-1} Z \triangleq EZ \quad (17)$$
$$E = (J^T R^{-1} J)^{-1} J^T R^{-1} \quad (18)$$

Estimated Z is given by $\hat{Z} = J\hat{X}$ (19)

The residual value r of the state estimator is the difference between observed measurement Z and the estimated measurement $\hat{Z}$and is given by $r = Z - \hat{Z} = (I - JE)Z$. Adding false value ΔZ to Z results in change in residual value. The *L-2 norm* of residual value is as follows

$$\|r^{new}\|_2 = \|Z + \Delta Z - JE(Z + \Delta Z)\|_2 \triangleq \|r\|_2 + \|(I - JE)\Delta Z\|_2 \quad (20)$$

In order to avoid being detected in the BDD procedure of ISO. The change in residual value (r^{new}) by adding compromised measurement ΔZ should be within the *threshold limit* $\|(I - JE)\Delta Z\|_2 \le \in$. This threshold limit is introduced as a constraint in the attacker's optimization problem.

IV. Optimal attack on Electricity Markets

Based on the state estimation and market clearing process, and in order to achieve the attacker's objective of profit maximization, the false data is injected into the network. these would create congestion in the desired transmission line, and for this the attacker must find out optimal generation and load values such that the attack is stealthy and passes through BDD procedure. In order to obtain optimal attack values, the attacker needs to relate DA and RT markets with the RTU's measurement data. For this the attacker considers network topology and physical constraints of both power markets in the attack problem. The attacker needs to choose some desirable meters that are to be compromised. Consequently, the attacker needs to embed the relation between the traded power $[P_{it}, D_{it}]$, DA and RT market LMPs i.e., $[LMP_{it}^{RT}, LMP_{it}^{DA}]$ and false data injected (through the RTU's). considering all the above issues, a bi-level false data injection attack strategy is proposed [2,15,17]. Let us define the $Z_{DA} = [P_{it}, D_{it}]$ are the DA market state variables and $Z_{RT} = [\Delta P_{it}, \Delta D_{it}]$ as the RT market state variables. The attacker's bi-level problem is interpreted as

$$\max_{\Delta P_{it},\Delta D_{jt}} Profit_{Att} = \sum_{i=1}^{\Omega_n}\sum_{t=1}^{T}\left[LMP_{it}^{RT}(\Delta P_{it} - \Delta D_{it}) + LMP_{it}^{DA}(P_{it} - D_{it})\right] \quad (21)$$

S.t

$$\sum_{m=1}^{M} U_{mt} \le C_{att} \qquad \forall m \in \Omega_l \quad (22)$$
$$\|(I - JE)\Delta Z_{mt}\|_2 \le \Delta\in \qquad \forall m \in \Omega_l \quad (23)$$
$$\Delta Z_{mt} + \Delta F_{lt} + F_{lt} - F_l^{max} \le 0 \qquad \forall ml \in \Omega_l;\ \vartheta_{mt}^a \quad (24)$$
$$\sum_{j=1}^{\Omega_d} \Delta D_{jt} = 0 \quad (25)$$
$$\frac{\Delta Z_{mt}}{F_l^{max}} \ge \sigma \qquad \forall m, l \in \Omega_l \quad (26)$$
$$\sum_{i=1}^{\Omega_g}(P_{it} - \Delta P_{it}) = \sum_{j=1}^{\Omega_d}(D_{jt} - \Delta D_{jt}) \quad (27)$$
$$\left[X_{DA}, \lambda_t, X_{RT}, \tilde{\lambda}_t\right] \in arg\,min\,(R_{DA} + R_{RT}) \quad (28)$$
$$S.t\begin{cases}(2)-(5)\\(8)-(12)\end{cases} \quad (29)$$

In the above bi-level optimization problem, Eq. (21) governs the attacker's objective of profit maximization. Eq. (22) represents, for any attack in a specific time slot, the attacker can compromise limited number of RTU's (meters) to a predefined number(C_{att}). In order to take care of not being detected by the ISO's BDD procedure the attacker tries to keep the FDI below the threshold limit ($\Delta\in$), this is shown in Eq. (23). Eq. (25) represents total change in the demand values should be equal to zero. The injected false data can cause overloading level greater than a given threshold value(i.e.), which can be ensured by constraint in Eq. (26). Eq. (27) puts constraint on the amount of traded power in DA should be equal to RT markets. Eq. (24) ensures the injected false data follows KCL for power flows at a node. Eqs. (28) and (29) represents the lower level market clearing problem discussed in the section II. The main aim behind considering the market clearing problem is to mislead the process and remain undetected by the ISO. Due to this the attacker's decision-making problem turn in to bi-level optimization problem. In the next section, [22-23] using KKT conditions and strong duality constraints, the set of equations in the lower level problem can be turned in to MILP problem. Therefore, the above bi-level problem is turned in to single level MILP problem.

A. Bi-level to Single level MILP conversion

In simplifying bi-level optimization problem, Karush-Kuhn-Tucker optimality conditions for multivariable inequality constrained optimization technique is used. The lower level problem is a convex optimization problem on its decision variables [22]. Therefore, the market clearing problem of both DA and RT markets can be replaced by the

KKT optimality conditions. Moreover, the complementary slackness can be linearized using big M-method. This procedure is clearly explained in [23,24].
The KKT optimality conditions of the lower level market clearing problem is as follows

$$C_{it} - \lambda_t + \mu_{it}^{max} - \mu_{it}^{min} + \sum_{l\in\Omega_n} S_{li}\left(\vartheta_{it}^{max} - \vartheta_{it}^{min}\right) = 0 \tag{30}$$

$$-B_{it} + \lambda_t + \gamma_{it}^{max} - \gamma_{it}^{min} - \sum_{l\in\Omega_n} S_{li}\left(\vartheta_{it}^{max} - \vartheta_{it}^{min}\right) = 0 \tag{31}$$

$$C_{it} - \tilde{\lambda}_t + \tilde{\mu}_{it}^{max} - \tilde{\mu}_{it}^{min} + \sum_{l\in Cl_+} S_{li}\left(\tilde{\vartheta}_{it}^{max} - \tilde{\vartheta}_{it}^{min}\right) = 0 \tag{32}$$

$$-B_{it} + \tilde{\lambda}_t + \tilde{\gamma}_{it}^{max} - \tilde{\gamma}_{it}^{min} - \sum_{l\in Cl_-} S_{li}\left(\tilde{\vartheta}_{it}^{max} - \tilde{\vartheta}_{it}^{min}\right) = 0 \tag{33}$$

$$0 \le P_{it}^{max} - P_{it} \le M(1 - \overline{U}_{it}) \tag{34}$$

$$0 \le \Delta P_{it}^{max} - \Delta P_{it} \le M(1 - \overline{U}_{it}) \tag{35}$$

$$0 \le \mu_{it}^{max} \le N(\underline{U}_{it}) \tag{36}$$

$$0 \le \tilde{\mu}_{it}^{max} \le N(\underline{U}_{it}) \tag{37}$$

$$0 \le D_{jt}^{max} - D_{jt} \le M(1 - \overline{U}_{jt}) \tag{38}$$

$$0 \le \Delta D_{jt}^{max} - \Delta D_{jt} \le M(1 - \overline{U}_{jt}) \tag{39}$$

$$0 \le \gamma_{jt}^{max} \le N(\underline{U}_{jt}) \tag{40}$$

$$0 \le \tilde{\gamma}_{jt}^{max} \le N(\underline{U}_{jt}) \tag{41}$$

$$0 \le P_{it} - P_{it}^{min} \le M(1 - \overline{U}_{it}) \tag{42}$$

$$0 \le \Delta P_{it} - \Delta P_{it}^{min} \le M(1 - \overline{U}_{it}) \tag{43}$$

$$0 \le \mu_{it}^{min} \le N(\underline{U}_{it}) \tag{44}$$

$$0 \le \tilde{\mu}_{it}^{min} \le N(\underline{U}_{it}) \tag{45}$$

$$0 \le D_{jt} - D_{jt}^{min} \le M(1 - \overline{U}_{jt}) \tag{46}$$

$$0 \le \Delta D_{jt} - \Delta D_{jt}^{min} \le M(1 - \overline{U}_{jt}) \tag{47}$$

$$0 \le \gamma_{jt}^{min} \le N(\underline{U}_{jt}) \tag{48}$$

$$0 \le \tilde{\gamma}_{jt}^{min} \le N(\underline{U}_{jt}) \tag{49}$$

$$0 \le F_{lt}^{max} - F_{lt} \le M(1 - \overline{U}_{lt}) \tag{50}$$

$$0 \le \vartheta_{lt}^{max} \le N(\underline{U}_{it}) \tag{51}$$

$$0 \le F_{lt} - F_{lt}^{min} \le M(1 - \overline{U}_{lt}) \tag{52}$$

$$0 \le \vartheta_{lt}^{min} \le N(\underline{U}_{it}) \tag{53}$$

$$0 \le \tilde{\vartheta}_{it}^{max} \le M(1 - U_{lt}) \tag{54}$$

$$-M(1 - U_{lt}) \le \sum_{i=1, l\in Cl_+}^{\Omega_n} S_{lj}\left(\sum_{i=1}^{\Omega_g} \Delta P_{it} - \sum_{j=1}^{\Omega_d} \Delta D_{jt}\right) \le 0 \tag{55}$$

$$0 \le \tilde{\vartheta}_{lt}^{min} \le M(1 - U_{lt}) \tag{56}$$

$$0 \le \sum_{i=1, l\in Cl_-}^{\Omega_n} S_{lj}\left(\sum_{i=1}^{\Omega_g} \Delta P_{it} - \sum_{j=1}^{\Omega_d} \Delta D_{jt}\right) \le M(1 - U_{lt}) \tag{57}$$

$$0 \le \vartheta_{lt}^{a} \le M(U_{mt}) \tag{58}$$

$$-M(U_{lt}) \le \Delta Z_{mt} + \Delta F_{lt} + F_{lt} - F_l^{max} \le 0 \tag{59}$$

Where $U_{it}, U_{jt}, U_{lt} \in \{0,1\}; (\forall\, i,j \in \Omega_g, \Omega_d;\ \forall l \in \Omega_l)$, M and N are large positive integer values. Equalities from Eq. (30) to Eq. (33) are obtained by taking derivatives of the Lagrange function of the lower level problem with respect to the decision variables and are defined over $\forall i \in \Omega_n$. Constraints from Eq. (34) to Eq. (54) are the linearized complementary constraints regarding inequalities in the Eqs. (3)-(5) and Eq. (9)-(10). Eqs. (55) to (59) are the attacker's constraints. If the attacker wants to attack any meter, then the faked eqs. (58) and (59) are injected into the problem as explained in [17]. The attacker's objective function i.e. Eq. (21) is a non-linear function. [22] Using Eqs. (30) to (33), we linearize the Eq. (21). Therefore, the resultant single level MILP problem is as follows.

Obj:
$$\max_{\Delta P_{it}, \Delta D_{jt}} Profit_{Att} = C_{it}P_{it} + \mu_{it}^{max}P_{it}^{max} - \mu_{it}^{min}P_{it}^{min} - B_{it}D_{it} + \gamma_{it}^{max}D_{it}^{max} - \gamma_{it}^{min}D_{it}^{min} + C_{it}\Delta P_{it} + \tilde{\mu}_{it}^{max}\Delta P_{it}^{max} - \tilde{\mu}_{it}^{min}\Delta P_{it}^{min} - B_{it}\Delta D_{it} + \tilde{\gamma}_{it}^{max}\Delta D_{it}^{max} - \tilde{\gamma}_{it}^{min}\Delta D_{it}^{min} \tag{60}$$

$$\text{S.t} \begin{cases} upper\ level\ constraints\ Eq.(22) - Eq.(27) \\ KKT\ optimality\ constraints\ Eq.(30) - Eq.(54) \\ attacks\ own\ constraints\ Eq.(55) - Eq.(59) \end{cases} \tag{61}$$

V. Simulation Results

The proposed methodology is implemented on PJM-5 bus system to empirically investigate the impact of financially motivated FDI attacks. The relevant data is taken from the MATPOWER packages.

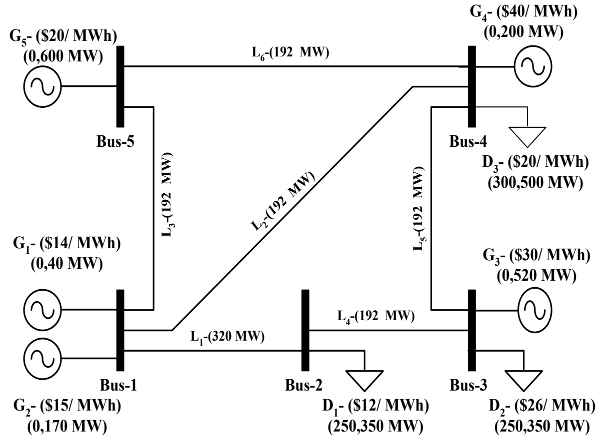

Fig. 1. PJM-5 Bus system.

As shown in Fig. 1, the PJM-5 bus system consists of 5 generation meters, 3 load meters, and 6 branch flow meters. As Power system is usually a vast network, operates with different zones, and will have different communication lines to send data to the system operator, it is difficult for an attacker to attack the entire system. For any FDI attack, the attacker needs to estimate network parameters including transmission line parameters and thermal limits. The results for six different scenarios in which attack on five-line flow meters are illustrated in Fig.2 and Fig.3. In each case the attacker can compromise two meters, the attacker has the provision of attacking more meters but in the present case, the attacker is limited to attack two meters. Load forecast error is small, the injected fake data at the loads are limited to $\tau = 0.05$, and change in line flow limits is set to $\sigma = 0.5$. The large positive values M and N are set to 5×10^4 and 1×10^4 respectively. The proposed financially motivated FDI attacks are implemented in GAMS software using

CLPEX solver on a PC with an Intel i5 3.6GHZ CPU and 8-GB RAM.

A. Financial investigation of the attack on meters (RTU's):

In this section, change in LMPs during different attack scenarios is demonstrated, there are 6 potential line flow meters and all the meters can be compromised. Under no attack condition. Line-6 is congested between buses 4 and 5. The participant(attacker) in the market buy power from cheap generating stations in the DA market and sell it for higher prices in the RT market. For example, a market participant(attacker) wants to make profits, buys 24MW of power at 31.61 ($/ MW h) from generating plant-5 at bus-5 in the DA market and sells the same amount of power at different bus numbers wherever LMP is high. It is assumed that the participant (attacker) sells the power at bus-1 at 49($/ MWh). The total profit gained by the attacker is $24MW\ (49 - 31.61)\ \$/MWh\ = 417.39\$/hr$. So, behind any attack made by the attacker, there is financial motivation. In order to successfully launch finically motivated FDIs the attacker need to change the congestion pattern in the system. This can be achieved by compromised power flow meters. Therefore, for any attack in a time period, the attacker needs to run the optimization problem in Eqs. (60) – (61).

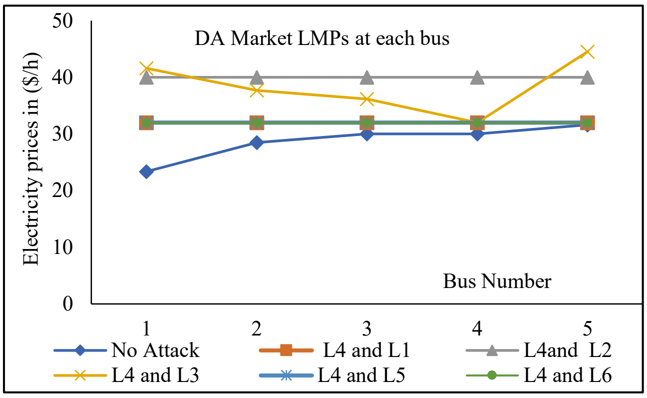

Fig. 2. Electricity Market prices (LMPs) in DA market with and without attack at individual bus number for 6 scenarios (L4-L1, L4-L5 are super imposed with L4-L6)

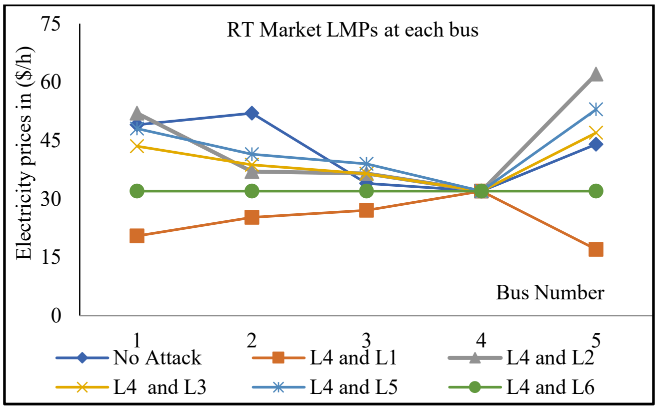

Fig. 3. Electricity Market prices (LMPs) in RT market with and without attack at individual bus number

In the first case the attacker compromise line-4 and line-1 meters. As a result, the congested line-6 between bus 4 and 5 is relived and there is no congestion in the system. This leads to the same LMPs at every bus. Similarly, in another case when the attacker tries to compromise line-4 and line-3 meters, it is observed that line-6 is again congested, as a result, there will be different LMP's at each bus as shown in Fig.2. Hence during this attack, the attacker buys power in DAM and sells in RTM. Power flow meter values with and without attack are presented in Table-II. Based on the LMP's in the DA market the attacker decides to buy/sell the power in the RT. In most cases, the attacker tries to remove congestion in the DA market, in order to mitigate the risk of getting financial loss. From Fig. 3 it can be observed that under the attack by compromising line-4 and line-1 meters, the attacker will obtain loss as the difference between DA and RT market prices is negative. During this period the attacker tries to sell his power at bus-4 in the RT market as LMPs are the same in both markets. Here the attacker is out of risk from financial losses.

When the attacker tries to compromise line-4 and line-2 meters in the DA market, the LMPs at each bus are same but higher compared to the other. In this case, the attacker compromised the meters such that the generator-4 which is costly compared to the other generators are made to dispatch. Consequently, in the RT market during the same attack, the LMP's at each bus are higher compared to the other cases. This provides proof for the best-attacking strategy. Also, it can be observed that the attacker needs to compromise line-4 meter for every attack in order to obtain optimal attack vector and from Fig. 2 and Fig. 3 it can be observed that change in LMP's at bus-4 in both DA and RT market is very less compared to the other variations in the LMP's. This provides a chance for the attacker to avoid the risk of getting financial loss.

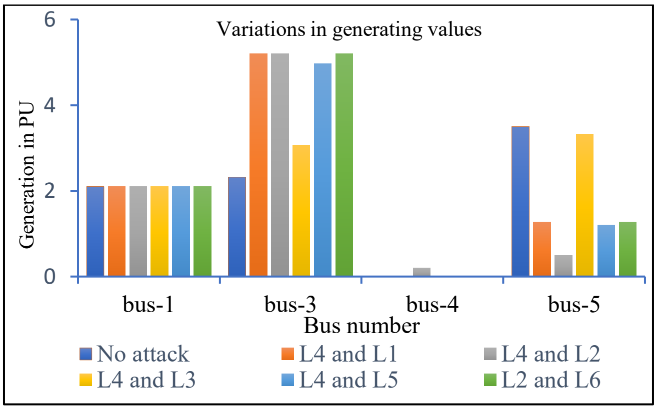

Fig. 4. Electricity generation under attack and no attack conditions (base value = 100MW)

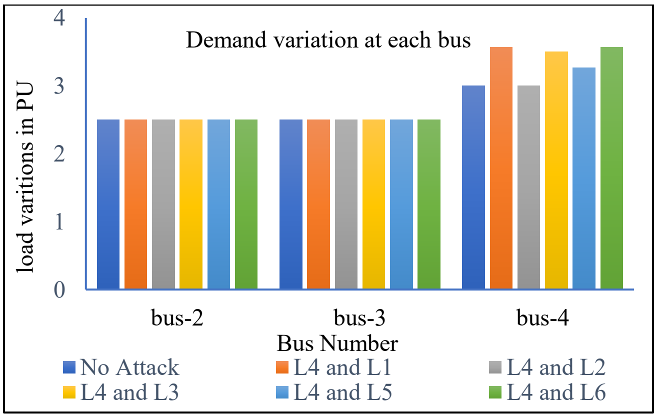

Fig. 5. Electricity Demand values under attack and no attack condition

The generation and demand variations in the DA market are depicted by Figs.4, 5 respectively. The generation at bus-1 under no-attack and attacking conditions are the same. But, under the attack conditions, the generation at bus-3 and bus-5 are varied. This reveals that the generating meters at bus-3 and bus-5 are more vulnerable compared to the meters at bus-1 and bus-4. This shows that the attacker prefers to buy/sell power at these buses more often compared to other meters to gain financial benefits.

TABLE II. POWER FLOW METERS (MW) UNDER ATTACK AND NO ATTACK CONDITIONS

C_{att}	L_1	L_2	L_3	L_4	L_5	L_6
No Attack	222.8	152.71	-165.60	-27.107	-44.714	-192.00
L_4-L_1	85	124.25	0	-164.25	105.74	-127.14
L_4-L_2	73.32	96.23	40.44	-176.67	93.32	-89.73
L_4-L_3	192	157.95	-140.76	-57.18	0	-192
L_4-L_5	92.44	117.55	0	-157.55	90.11	-120.28
L_4-L_6	85	124.25	0	-164.25	105.74	-127.14

The demand variations at bus-2 and bus-3 are seen for both attacking conditions. So, the attacker may prefer to buy at these buses. But the change in the demands is observed at bus 4, here the attacker tries to buy the power at this bus. It has transpired from the above scenarios that the attacker will be interested to compromise the flow meters of line-3, line-5, and line-6 along line-4. All these lines form node at bus 4. Hence bus-4 is more vulnerable to the attack. Compromising the above meters in the specified combination will result in financial profits in each case. The presented model can be extended to attack more than two meters. This increases the change in error in Eq. (23). As a result, the probability of launching a stealthy attack may be reduced.

VI. CONCLUSION

In this paper, model of cyber-attack to the electricity markets considering PJM- 5-bus system has been formulated and investigated with manipulation of RTU's data as a MILP problem. The attacker has been considered as a virtual bidder in the market, and the attacker's objective of profit maximization has been realized considering ISO market-clearing problems in DA as well as RT markets. The simulation results have explicitly revealed the dependency of market prices on state variables and false data and exposed the weak points in the system (as in the above results line flow meter. It has transpired that the attacker leads the market-clearing problem to gain consistent financial benefits. This provides the system operator to improve the security at vulnerable points. However, appropriate mitigation strategies along with the study on the sensitivity of state estimation will be taken up as future work.

REFERENCES

[1] Y. Liu, P. Ning, and M. K. Reiter, "False data injection attacks against state estimation in electric power grids," *ACM Trans. Inf. Syst. Security*, vol. 14, no. 1, pp. 1–33, 2011

[2] H. Wang et al., "Dynamic Data Injection Attack Detection of Cyber Physical Power Systems With Uncertainties," in *IEEE Transactions on Industrial Informatics*, vol. 15, no. 10, pp. 5505-5518, Oct. 2019, doi: 10.1109/TII.2019.2902163.

[3] M. Esmalifalak, L. Liu, N. Nguyen, R. Zheng, and Z. Han, ``Detecting stealthy false data injection using machine learning in smart grid," *IEEE Syst. J.*, vol. 11, no. 3, pp. 1644_1652, Sep. 2017.

[4] M. Esmalifalak, L. Liu, N. Nguyen, R. Zheng, and Z. Han, ``Detecting stealthy false data injection using machine learning in smart grid," *IEEE Syst. J.*, vol. 11, no. 3, pp. 1644_1652, Sep. 2017.

[5] A. Ameli, A. Hooshyar, E. F. El-Saadany, and A. M. Youssef, ``Attack detection and identi_cation for automatic generation control systems," *IEEE Trans.Power Syst.*, vol. 33, no. 5, pp. 4760_4774, Sep. 2018.

[6] H. Sedghi and E. Jonckheere, ``Statistical structure learning to ensure data integrity in smart grid," *IEEE Trans. Smart Grid*, vol. 6, no. 4, pp. 1924_1933, Jul. 2015.

[7] Q. Yang, J. Yang, W. Yu, D. An, N. Zhang, and W. Zhao, `` false data-injection attacks against power system state estimation: Modeling and counter measures," *IEEE Trans. Parallel Distrib. Syst.*, vol. 25, no. 3, pp. 717_729, Mar. 2014.

[8] J. Yan, Y. Tang, B. Tang, H. He, and Y. Sun, ``Power grid resilience against false data injection attacks," *IEEE Power Energy Soc. Gen. Meeting (PESGM)*, Boston, MA, USA, Nov. 2016, pp. 1_5.

[9] R. Deng, G. Xiao, R. Lu, H. Liang and A. V. Vasilakos, "False Data Injection on State Estimation in Power Systems—Attacks, Impacts, and Defense: A Survey," in *IEEE Transl Informatics*, vol. 13, no. 2, pp. 411-423, April 2017, doi: 10.1109/TII.2016.2614396.

[10] J. Zhao, G. Zhang, Z. Y. Dong and K. P. Wong, "Forecasting-Aided Imperfect FDIAs Against Power System Nonlinear State Estimation," in *IEEE Transactions on Smart Grid,* vol. 7, no. 1, pp. 6-8, Jan. 2016.

[11] Y. Yuan,etal "Modelling load redistribution attacks in power systems," *IEEE Trans. Smart Grid*, vol. 2, no. 2, pp. 382–390, Jun. 2011.

[12] X. Liu, Z. Li, Z. Shuai, and Y. Wen, "Cyber attacks against the economic operation of power systems: A fast solution," *IEEE Trans. Smart Grid*, vol. 8, no. 2, pp. 1023–1025, Mar. 2017.

[13] L. Xie, Y. Mo, and B. Sinopoli, "Integrity data attacks in power market ," *IEEE Trans. Smart Grid*, vol. 2, no. 4, pp. 659–666, Dec. 2011.

[14] L. Jia, et.al "Impacts of malicious data on real-time price of electricity market operations*," in Proc. HICSS*, 2012, pp. 1907–1914.

[15] D. Choi and L. Xie, "Economic Impact Assessment of Topology Data Attacks With Virtual Bids," in *IEEE Transactions on Smart Grid*, vol. 9, no. 2, pp. 512-520, March 2018, doi: 10.1109/TSG.2016.2535246.

[16] C. Liu, M. Zhou, J. Wu, C. Long and D. Kundur, "Financially Motivated FDI on SCED in Real-Time Electricity Markets: Attacks and Mitigation," in IEEE Transactions on Smart Grid, vol. 10, no. 2, pp. 1949-1959, March 2019, doi: 10.1109/TSG.2017.2784366.

[17] X. Liu, Y. Song and Z. Li, "Dummy Data Attacks in Power Systems," in *IEEE Transactions on Smart Grid*, vol. 11, no. 2, pp. 1792-1795, March 2020, doi: 10.1109/TSG.2019.2929702.

[18] S. Ahmadian, X. Tang, H. A. Malki and Z. Han, "Modelling Cyber Attacks on Electricity Market Using MPEC," in IEEE Access, vol. 7, pp. 27376-27388, 2019, doi: 10.1109/ACCESS.2019.2899293.

[19] L. Xie, Y. Mo and B. Sinopoli, "Integrity Data Attacks in Power Market Operations," in *IEEE Trans on Smart Grid*, vol. 2, no. 4, pp. 659-666, Dec. 2011, doi: 10.1109/TSG.2011.2161892.

[20] A. Tajer, "False Data Injection Attacks in Electricity Markets by Limited Adversaries," in *IEEE Trans on Smart Grid*, vol. 10, no. 1, pp. 128-138, Jan. 2019, doi: 10.1109/TSG.2017.2733346.

[21] A. Kundu, A. Sahu, K. Davis and E. Serpedin, "Learning-Based Defense of FDIAs in Power System State Estimation," *2019 North American Power Symposium (NAPS),* Wichita, KS, USA, 2019, pp. 1-6, doi: 10.1109/NAPS46351.2019.9000216

[22] Ganjkhani, M, Fallah, S, Badakhshan. S, Shamshirband. S, Chau, K. "A Novel Detection Algorithm to Identify FDIAS on Power System State Estimation", *Energies 2019*, 12(11), 2209

[23] Luis Baringo, Morteza Rahimiyan, "Virtual Power Plants and Electricity Markets Decision Making Under Uncertainty", Springer Nature March.2020

[24] Jonathan F. Bard, "Practical Bilevel Optimization: Algorithms and Applications, *Algorithms and Application",* e-book ,*Texas,* Volume 30, DOI 10.1007/978-1-4757-2836-1.

[25] Steven A.Gabriel, Antonio J.Conejo, J.David Fuller ,Benjamin F.Hobbs, Carlos Ruiz, "Complementarity Modelling in Energy Markets", DOI 10.1007/978-1-4419-6122-8 -6123-

6th International Conference for Convergence in Technology (I2CT)

2nd – 4th April 2021

Certificate

This is to certify that Dr./Prof./Mr./Ms. R.S Saha Affiliation Delhi Technological University has participated in 6th International Conference for Convergence in Technology (I2CT) during 2nd to 4th April 2021.

He / She presented a technical paper titled Two-Stage Stochastic Programming Model for Optimal Scheduling of RES-Based Virtual Power Plants in Electricity Market.

Dr. Chanakya Kumar Jha
General Chair -I2CT

ICPECTS'20

ARIIA TOP 25 RANKING INSTITUTION | nirf 108 RANK | SUSTAINABLE DEVELOPMENT GOALS

Sri SAI RAM ENGINEERING COLLEGE

An Autonomous Institution | Affiliated to Anna University & Approved by AICTE, New Delhi

Accredited by NBA and NAAC "A+" | An ISO 9001:2015 Certified and MHRD NIRF ranked institution

Sai Leo Nagar, West Tambaram, Chennai - 600 044. www.sairam.edu.in

Department of Electrical & Electronics Engineering

VIRTUAL IEEE INTERNATIONAL CONFERENCE ON POWER, ENERGY, CONTROL AND TRANSMISSION SYSTEMS

10.12.2020 & 11.12.2020

Best Paper Award

This is to certify that the paper titled Modelling Financially Motivated Cyber Attacks on Electricity Markets Using Mixed Integer Linear Programming

presented by Dr./Mr./Ms. Radheshyam Saha

of Delhi Technological Univesity has been adjudged as **BEST PAPER** in the

IEEE International Conference on "Power, Energy, Control and Transmission Systems" held at Sri Sairam Engineering College, Chennai, Tamil Nadu, India on 10th and 11th December 2020.

Dr. C. Nayanatara **Ms. P. Shanmugapriya** Conference Chairs	**Dr.T . Porselvi** HOD/EEE	**Dr. A. Rajendra Prasad** Principal	**Sai Prakash LeoMuthu** Chairman & CEO

Technical Co-Sponsor

IEEE young professionals Power & Energy Society | IEEE Madras Section | IEEE PES Power & Energy Society SSEC Student Branch Chapter

Sairam INSTITUTIONS www.sairamgroup.in

6th International Conference for Convergence in Technology (I2CT)

IEEE BOMBAY SECTION

2nd – 4th April 2021

Certificate

This is to certify that Dr./Prof./Mr./Ms. Radheshyam Saha Affiliation Delhi Technological University has participated in 6th International Conference for Convergence in Technology (I2CT) during 2nd to 4th April 2021.

He / She presented a technical paper titled An Adaptive Master-Slave Technique using Converter Current Modulation in VSC-based MTDC System.

Dr. Chanakya Kumar Jha
General Chair -I2CT

Advisory Committee

Prof. Bhim Singh, IIT Delhi
Prof. K. Gopakumar, IISc Bangluru
Prof. Subrata Mukhopadhyay, IEEE-Delhi
Er. Gurdeep Singh, MD NTPC
Prof. Sukumar Mishra. IIT Delhi
Er. Tarini Baswal, IRES
Prof. Madhusudan, DTU Delhi
Prof. D. K. Jain, DCRUST Murthal
Prof. Narendra Kumar-I, DTU Delhi
Prof. Vishal Verma, DTU Delhi
Prof. Pragati Kumar, DTU Delhi
Er. Satnam Singh, NHPC
Prof. Narendra Kumar-II, DTU Delhi
Er. Vijender Chaudhary, DMRC
Prof. Rachna Garg, DTU Delhi
Prof. Suman Bhowmick, DTU Delhi
Prof. Bharat Bhushan, DTU Delhi
Prof. S. T. Nagrajan, DTU Delhi
Prof. Alka Singh, DTU Delhi
Prof. Dheeraj Joshi, DTU Delhi
Prof. M. M. Tripathi, DTU Delhi
Prof. J. N. Rai, DTU Delhi
Prof. Priya Mahajan, DTU Delhi
Er. Manu Jain, SIEMENS India

Organizing Committee

Er. N. K. Bhagat
Er. Ram Bhagat
Dr. Mini Sreejeth
Dr. Vinod K. Yadav
Er. Prem Prakash
Er. A. B. K. Bhattacharya
Er. Garima
Er. Bhavnesh Jaint
Er. A. R. Kulkarni
Dr. Anup Kumar Mandpura
Er. Sikandar Ali Khan
Er. Himanshu
Er. Kuldeep Singh
Er. Ankita Arora
Er. Saurabh Mishra

Patron in Chief
Prof. Yogesh Singh
Hon'ble Vice- Chancellor, DTU

Patrons
Prof. S. K. Garg, Pro-VC, DTU
Prof. Uma Nangia, HOD EED, DTU

Coordinator
Prof. Mukhtiar Singh
mukhtiarsingh@dce.ac.in
8901073179, 8178608809

Co-Coordinators
Prof. R. Saha
Dr. S. K. Valluru
Sh. D. C. Meena

Volunteers

Er. Aakash Seth
Er. Ashima Taneja
Er. Kailash Rana
Er. Nimmi
Er. Rupam Singh
Er. Pallavi Verma
Er. Saket Gupta
Er.Avdesh Kumar
Er. Pankhuri Asthana
Er. Suryakant
Er. Ajishek
Er. Hemant Saxena
Er. Astitva Kumar
Er. Aditya Narula
Er. Mohd. Bilal
Er. Shirish Raizada
Er. Snigdha Sharma
Er. Monika Verma

Sponsorship Opportunity

The leading industries/organization may participate in the workshop through sponsorship program in the following categories:

Platinum Sponsorship	Rs. 200,000/-
Gold Sponsorship	Rs. 150,000/-
Silver Sponsorship	Rs. 100,000/-

IEEE

Workshop & Exposition On Grid Integrated Renewables & Electric Transportation

17 – 18th Dec. 2019

Organized By
Department of Electrical Engineering
Delhi Technological University
Delhi-110042

Chief Guest

Distinguished Speakers

Prof. Tarlochan S. Sidhu, UOIT, Canada
Prof. Ambrish Chandra, ETS, Canada
Prof. Sheldon Williamson, UOIT, Canada
Dr. Subir Sen, Power Grid
Er. Tarini Baswal, IRSEE, COFMOW
Er. Tilak Raj Seth, SIEMENS India Ltd.
Prof. Mukhtiar Singh, DTU Delhi

About Workshop

Electric power systems are perhaps the largest and most complex human engineered systems. Recently, the worldwide power system networks are facing huge challenges in terms of grid integration of intermittent renewables and incorporation of electric transportation/EV charging infrastructure. However, with advancement in digital control & protection, together with exciting innovations in power electronics and energy storage, the power engineers are better equipped to manage operation of the grid and electric propulsion transportation systems simultaneously. Thus, the main aim of the proposed workshop is to provide a platform to the budding engineers and researchers to take the maximum benefit out of the expertise of distinguished speakers working in the frontal areas of Digital control & protection, transport electrification, grid integration of Renewables and electric vehicle charging infrastructure.

Registration Form

Name :

Designation :

Organization :

Address :

Mob. No. :

Email ID :

About DTU

"75 years of Tradition of excellence in Engineering & Technology Education, Research and Innovations" Delhi College of Engineering, (initially established with the name – Delhi Polytechnic) came into existence in the **year 1941** to cater the needs of Indian industries for trained technical manpower with practical experience and sound theoretical knowledge. In 1952 the college was affiliated with University of Delhi and started formal Degree level Programmes. Delhi College of Engineering is the mother institution of a number of national projects including IIT Delhi, School of planning and Architecture, Delhi, College of Arts and even the famous FMS, Delhi. In 1963 the college was handed over to Govt. of NCT Delhi, which further upgraded it to Delhi Technological University, Delhi in 2009.

About Department

The department of electrical engineering has earned the reputation of Centre for excellence in academic research and development. Thanks to its highly educated and dynamic faculty which have the global exposure and have the expertise in the emerging areas of electrical engineering. The electrical engineering department currently offers two Bachelor and two Masters programs besides Ph.d in the major areas of power system, control system, power electronics & drives and renewable energy sources.

Prof. Tarlochan S. Sidhu is Professor and Dean of Faculty of Engineering, University of Ontario Institute of Technology (UOIT), Oshawa, ON, Canada. He is fellow of IEEE (USA), IEE/IET (UK), CAE (Canada).

Prof. Ambrish Chandra is Professor at École de Technologie Supérieure (ETS), Universié du Québec, Montréal, Canada. He is fellow of IEEE (USA), IEE/IET (UK).

Prof. Sheldon S. Williamson is Professor at UOIT, Canada. He is also NSERC, Canada Research Chair in Electric Energy Storage Systems for Transportation Electrification.

Dr. Subir Sen is Chief Operating Officer (CTU Planning and Smart Grid) at PGCIL. He has vast experience in the area of power system planning, operation and control.

Er. Tarini Baswal is IRSEE and presently serving as Chief Electrical Engineer at COFMOW, Indian Railways. She had been the General Manager of Centre For Railway Information Systems (CRIS).

Er. TILAK RAJ SETH is Executive Vice-President of **Siemens** and Chief Executive Officer of its mobility division in India. He has vast experience in E-Mobility.

Prof. Mukhtiar Singh is with Delhi Technological University, Delhi. His research areas includes, RES, Microgrid and Electric Vehicle.

Registration Fee:

Faculty Member/Academician	Rs. 1000/-
Industrial Delegates	Rs. 2000/-
IEEE Members	Rs. 500/-
Students/Research Scholars	Rs. 500/-

The registration fee may be paid in cash or through DD drawn in favour of Registrar, Delhi Technological University, Delhi

Declaration By the Participant

The information furnished above is true to the best of my knowledge and agreed to abide the rules & regulations governing the program.

Date: Signature of Applicant

Note:

An exhibition of products/projects undertaken by students is also planned where they will be awarded for three best products/projects. Accordingly, the students from different institutes are encouraged to participate.

Ref. No. DTU/DEE/PQFDP/SPK2

Department of Electrical Engineering
Delhi Technological University

(Formerly Delhi College of Engineering)
Bawana Road, Delhi (110042)

CLARIANT FRAKO
In collaboration with Frako-Germany

CERTIFICATE OF PARTICIPATION

This certificate is granted to

Prof. RS Saha

From Delhi Technological University, Delhi

In recognition of delivering an expert lecture on ***"Reactive Power Compensation and Control",*** in Online Faculty Development Programme on "***Power Quality and Reactive Power Management***", organized by the Department of Electrical Engineering, Delhi Technological University, Delhi in association with Clariant Power System Ltd., Pune, during 06th -10th July 2020.

Mr. Baldev Raj Narang	Prof. Uma Nangia	Dr. Prakash Chittora	Dr. Rinchin W. Mosobi
CEO, Clariant Power System Ltd.	HOD, DEE, DTU	Course Coordinator, DEE, DTU	Course Coordinator, DEE, DTU

OPJU

OP JINDAL UNIVERSITY ESTD. 2014

UNIVERSITY OF STEEL TECHNOLOGY AND MANAGEMENT

Certificate No. OPJU/EED/FDP/ETPEPS-2020/ EX11

Date:- 01/09/2020

One Week online Faculty Development Programme on

"EMERGING TRENDS IN POWER ELECTRONICS AND POWER SYSTEM" (ETPEPS-2020)

(August 24-29, 2020)

Organized By

Department of Electrical Engineering

O P JINDAL UNIVERSITY, RAIGARH (CG)

Certificate of Appreciation

This is to certify that Mr./Ms./Dr ***PROF.(DR.) RADHEYSHYAM SAHA***

from ***DETLHI TECHNOLOGICAL UNIVERSITY, DELHI, INDIA***

has **delivered expert lecture** in the Faculty Development Programme on **"Emerging Trends in Power Electronics and Power System"** held from 24-29 August, 2020 in online mode organized by Department of Electrical Engineering, O P Jindal University, Raigarh, Chhattisgarh, India.

Dr. Deepak Singh
Convener

Dr. Sandeep Biswal
Convener

Dr. Imran Ahmad Quadri
Convener

Dr. Srikant Prasad
Chairman

Dr. R. D. Patidar
Vice Chancellor

Scan QR code to verify the certificate

DESIGN AND MODELING OF A FILTER ASSISTED 6-PULSE VSC-IGBT BASED D-STATCOM FOR REACTIVE POWER COMPENSATION

Biswabijet Panigrahy
Dept. of Electrical Engineering
Delhi Technological University
Delhi, India
Email: biswabijet20@gmail.com

Bushra Arif
Dept. of Electrical Engineering
Delhi Technological University
Delhi, India
Email: bushra75arif@gmail.com

Ritul Panchal
Dept. of Electrical Engineering
Delhi Technological University
Delhi, India
Email: ritulpanchal2709@gmail.com

Radheshyam Saha
Dept. of Electrical Engineering
Delhi Technological University
Delhi, India
Email: rshahacno@yahoo.com

Krishna Dutt
Dept. of Electrical Engineering
Delhi Technological University
Delhi, India
Email: krishna@dtu.ac.in

***Abstract*— Utilities are looking for cost-effective solutions to improve the grid's power quality and stability. Applications of FACTS devices provide a popular and proven solution to reactive power compensation, mitigating grid instability, improving power quality and voltage stability. Amongst a plethora of FACTS devices, shunt controllers are the most sought-after power controllers in which the power electronics-based Static Synchronous Compensators or STATCOM is the popular state-of-the-art technology. The increasing penetration of distributed RE (DRE) based electricity generation plays a crucial role in supplying power to loads in remote areas, especially where the main grid system is inaccessible. Such areas are frequently suffering the problems of reliable power supply, power quality, and voltage instability. The Utilization of smart inverters based on dynamic reactive power compensation by Distributed-STATCOM (D-STATCOM) has enabled to qualitatively improve the end-user requirements in the electricity distribution system. The design and behavior of a simple filter assisted D-STATCOM for reactive power compensation during variation of inductive loads is the topic of this paper. A cost-effective ±200kVAr D-STATCOM armed with a novel output filter and improved PI controller employing the pulse width modulated (PWM) technique to IGBT based Voltage Source Converter is proposed to compensate reactive power requirement of loads and to improve transient and dynamic stability, limiting harmonic distortion within standard IEEE-519 limits. The proposed STATCOM design is simulated in Simulink/MATLAB, which confirms its satisfying dynamic reactive power compensation capabilities and low level of harmonic distortion.**

Keywords—FACTS, D-STATCOM, VSC, PI, reactive power compensation, PWM, DRE, TDD

I. INTRODUCTION

The majority of transmission networks today are AC networks, and some main characteristics of ideal AC grid networks include nominal system voltage, unity power factor, and smooth sinusoids of voltage and current[1]. Spikes, harmonics, notches, noise, voltage sags or swelling and flickers are the main power quality problems that are borne because of rush load, fast switching, lighting, etc. which in turn lead to perturbations in the AC grid. Therefore there is a profound necessity for power flow control in power systems[2]–[4].

FACTS controllers maintain voltage profile through reactive power compensation which leads to voltage regulation. The need for more transmission lines is minimized to exchange power economically and reliably in neighboring utilities [1]–[5].The primary objectives in distribution are voltage regulation for loads and power quality [7], [8].

STATCOM is an active and very fast acting shunt controller similar to a controllable reactive current source; its reactive current will rapidly follow changes in the load reactive current and automatically compensate the reactive power required by the grid system, meeting specific grid harmonic requirements.[1], [3], [8], [10]. Due to its DC-link capacitor, real power can be exchanged with the AC system by switching power converters with the support of an adequate DC power source. During a power outage, the STATCOM reacts rapidly by surging output that improves the real power transmitted to the consumer thus minimizing the post-fault effects. On fault clearance, reactive loads come back online and cause voltage sag which it responds rapidly by supplying the necessary reactive power to boost voltage and prevent under-voltage conditions. With STATCOM systems, grid operators gain fast accurate control of the reactive power all with minimal infrastructure investment and low environmental impact[8].The use of VSC opens the avenue for multilevel topologies, and increasing pulse order improves its features [11], [13]. For effective power controllability, near to the ideal fundamental frequency voltage is obtained by low pass filtering. It allows to manage both reactive and active power independently[13].

978-1-7281-8402-9/21/$31.00 ©2021 IEEE

II. Architecture And Operating Principle of STATCOM

The STATCOMS are utilized both in power transmission and distribution grids and categorized into T-STATCOMS and D-STATCOMS respectively. The D-STATCOM is rated up to 5MVAr [8], [10] and IGBTs are the matured technology being operated at PWM mode.

Generally, in a STATCOM as shown in Fig 2.1; Voltage Source Converter, DC-link capacitor, filter, and coupling transformer are the main components. As indicated in the single line diagram. STATCOM is connected as a shunt controller to a transmission system, where V_S is the voltage produced by a three-phase power supply, V_t is the voltage of the bus connected as an interface between STATCOM, Source and Load where V_{Sh} is the voltage generated by (STATCOM) generating as current I_{Sh} flowing through reactance X_t to supply or absorb reactive power as per Eq (2.1). The three voltage and current phasors are shown in Eq (2.2). The active power and reactive power to be generated by the compensator are defined in Eq (2.3) and Eq (2.4); the reactive power generated shall be meeting the load demand and active power should be almost zero (neglecting losses due to switching)[2], [3], [14].

$$I_{sh} = \frac{V_{Sh} - V_t}{jX_t} \tag{2.1}$$

$$\overline{V} = \begin{bmatrix} V_a \\ V_b \\ V_c \end{bmatrix}; \overline{V}_{Sh} = \begin{bmatrix} V_{aSh} \\ V_{bSh} \\ V_{cSh} \end{bmatrix}; \bar{I}_{Sh} = \begin{bmatrix} I_{Sha} \\ I_{Shb} \\ I_{Shc} \end{bmatrix} \tag{2.2}$$

$$P_{Sh} = -V_t V_{Sh} \cdot sin(\theta_t - \theta_{Sh}) / X_t \tag{2.3}$$

$$Q_{Sh} = V_t \, (V_{Sh} \cdot cos(\theta_t - \theta_{Sh}) - V_t) / X_t \tag{2.4}$$

$$\overline{V} - \overline{V}_{Sh} = R_{Sh}\bar{I}_{Sh} + L_{Sh}\frac{d\bar{I}_{Sh}}{dt} \tag{2.5}$$

$$V_d - V_{Sh\,d} = R_{Sh} \cdot I_{Sh\,d} + L_{Sh}\frac{dI_{Sh\,d}}{dt} - L_{Sh} \cdot \omega \cdot I_{Sh\,q} \tag{2.6}$$

$$V_q - V_{Sh\,q} = R_{Sh} \cdot I_{Sh\,q} + L_{Sh}\frac{dI_{Sh\,q}}{dt} - L_{Sh} \cdot \omega \cdot I_{Sh\,d} \tag{2.7}$$

The STATCOM design is based on controlling the power compensation ability of STATCOM by controlling the d-axis voltages and q-axis voltages [14] as depicted in Eq (2.6) and Eq (2.7).

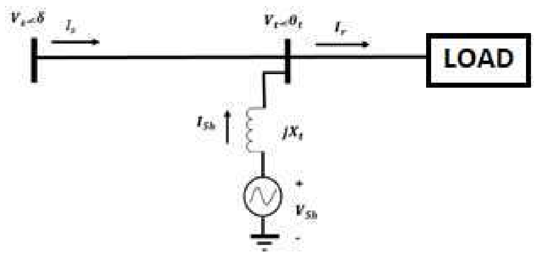

Fig. 2.1. Single line diagram of STATCOM in the transmission system

The STATCOM's V-I characteristics as shown in Fig 2.2 elucidates the degrees of compensation independence (in capacitive and inductive mode); which primarily depends on the AC-system voltage and the converter voltage. Over the rated maximum capacitive or inductive range, it can regulate its output current. Since it is capable of delivering a reactive current regardless of the network voltage, it can provide the highest inductive or capacitive current even at low voltage during sudden voltage collapse. The permissible converter's switches junction temperature regulates the device's transient rating in the inductive and area [1], [8], [14].

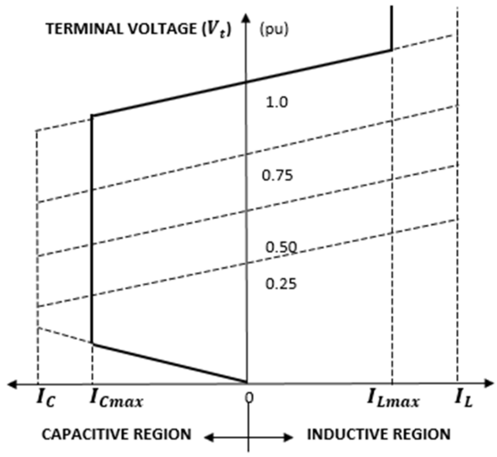

Fig. 2.2. V-I characteristics of STATCOM

The converter switches provide an interface for directly connecting the AC-output circuit to the DC-input circuit, thereby equalizing their net instantaneous power. The converter generates a circulating reactive-power that is exchanged among the phases. The power exchange occurs between the converter and systems' AC-terminals by utilizing the reactive power absorbed /or supplied by the capacitor[2], [3], [15].The DC capacitor not only provides circulating current paths but also provides a stiff voltage source. [2], [8]. The voltage difference between the voltage bus and the STATCOM determines reactive power exchange. The capacitor voltage is varied in order to change the amplitude of the output voltages as per the basic principles of STATCOM operation [2]. Thus, the magnitude and phase angle of the output voltage can be regulated.

PWM switching applied on IGBT converters can reduce harmonics. The output voltage can be regulated by varying voltage pulse width. The modulation frequency pushes the resulting harmonic content into the kHz range thereby making filter construction cost-effective. PWM can prevent fault current from entering the VSCs during transient conditions triggered by line faults. Therefore, the STATCOM can withstand AC transients without being blocked [5], [13].The fast switching action by supplying appropriate PWM gate signals and switching off through zero or negative gate signals makes IGBT easy to control and therefore used in D-STATCOMS [5], [8], [14]. The PWM signals fed into the convertor are generated by the control circuit which is driven by error signals which are controlled using PI controllers [17].

Fuzzy logic controllers (FLC) in combination with conventional PI-controllers are also used in STATCOM to obtain improved performance of the compensator. Such FLC does not require any mathematical formulation and is formulated based on rule based algorithm, linguistic variable and inference system guided by a set of membership functions [2], [18].

Among the various control strategies adopted in STATCOM [8] , the indirect current control theory (using instantaneous PQ theory) is chosen as the base algorithm to design the control circuit for D-STATCOM which involves direct-axis and quadrature-axis load current and voltage values for generating error signals under Phase Locked Loop control. The PLL is used for tracking the line frequency based on the PI controller and the Park's transformation. The stationary reference frame is used to obtain an accurate synchronization to the grid [5], [15].

III. DESIGN

IGBT is a combination of MOSFET topology with an insulated gate leading high voltage and current carrying capability. It is a majority carrier device which turns on by applying a positive base voltage to the channel. They are commutated by anti-parallel diodes, a bilayer fabrication of p-type and n-type semiconductors. It is a bi-terminal device that allows unidirectional current flow and blocks reverse currents. These are primarily used to rectify alternating current, suppress voltage spikes and have fast operation. Voltage ratings range from 50V-5kV and current ratings range from 1 A to 3500A [1]

The block model of the proposed filter assisted 6-pulse PWM VSC IGBT based ±200kVAr D-STATCOM design using indirect current control technique is presented in Fig. 3.1. The corresponding SIMULINK model for operating the device at grid frequency of 50 Hz is shown in Fig 3.2. The circuit design is comprising of four sections as depicted below.

1. Power Circuit:

This circuit consists of a 415V three phase AC supply connected with variable R-L load at the voltage bus which is connected to the STATCOM shunted by the LCL filter.

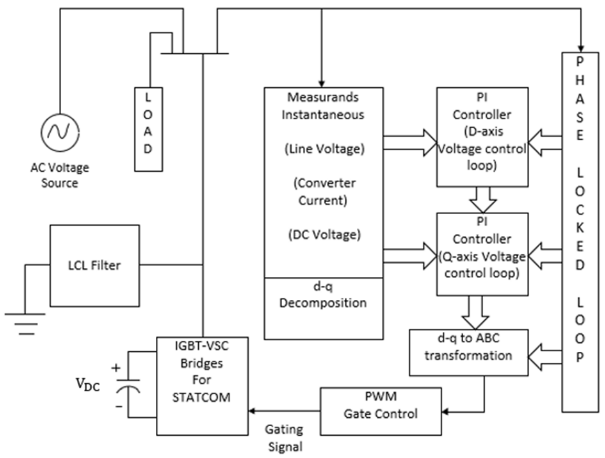

Fig. 3.1. D-STATCOM diagram using Indirect Current Control technique

a. Capacitor Design:

The capacitor voltage rating (V_{dc}) is calculated on the basis of maximum DC-bus voltage and PWM switching strategy to ensure low ripple currents using the following equations.

$$V_{DC} = \frac{2 \cdot V_{ll} \cdot \sqrt{2}}{m \cdot \sqrt{3}} \tag{3.1}$$

$$I_{RMS} = \frac{kVAr \times 10^3}{\sqrt{3} \times V_{ll}} \tag{3.2}$$

$$C = 0.6124 \times \frac{I_{RMS}}{f_{SW} \times \Delta V} F \tag{3.3}$$

where, V_{ll} (supply line voltage) = 415V, m=modulation index (84.7%), V_{dc}=800V, ΔV = ripple voltage (1%)

Using Eq (3.2), the rms current is calculated as 278 A for the proposed 200kVAr rated D-STATCOM.

Considering the safety margin, 1000V is chosen as the voltage rating of the DC bus. Using Eq. (3.3), where ΔV= ripple voltage= 1% of 800V=8V and f_{sw} = 10kHz (PWM switching frequency), and capacitor rating= 2130μF. Two 4260μF, 500V capacitors being readily available are considered in series [15].

b. LCL Filter Design:

The designing a low pass filter as LCL filter filters out high frequency harmonics, assuming current fluctuation of 8.5% on account of very low ripples produced by the D-STATCOM and a base capacitance (C_b) of 2000 μF. The design parameters are worked out by using the following equations:

$$I_{max} = I_{rms} \cdot \sqrt{2} \tag{3.3}$$

$$\Delta I_{Lmax} = 8.5\% \cdot I_{max} \tag{3.4}$$

$$L_1 = \frac{V_{DC}}{6 \cdot f_{sw} \cdot \Delta I_{Lmax}} \tag{3.5}$$

$$C_f = 0.05 \cdot C_b \tag{3.6}$$

As per the calculation I_{max}=393.15A; ΔI_{Lmax}= 33.418A; With these values, inductance connected to the converter (L_1 = 500 micro henry) and filter capacitance (C_f = 100 μF) are calculated.

$$\omega_{res} = \sqrt{\frac{L_1 + L_2}{L_1 \cdot L_2 \cdot C_f}} \; ; \quad f_{res} = \frac{\omega_{res}}{2\pi} \; ; \tag{3.7}$$

$$10 f_g < f_{res} < 0.5 f_{sw} \tag{3.8}$$

The value of L_2 (inductor connected to voltage bus) is calculated to be 272μF using Eq 3.7 and frequency limitations as presented in Eq 3.8 [19].

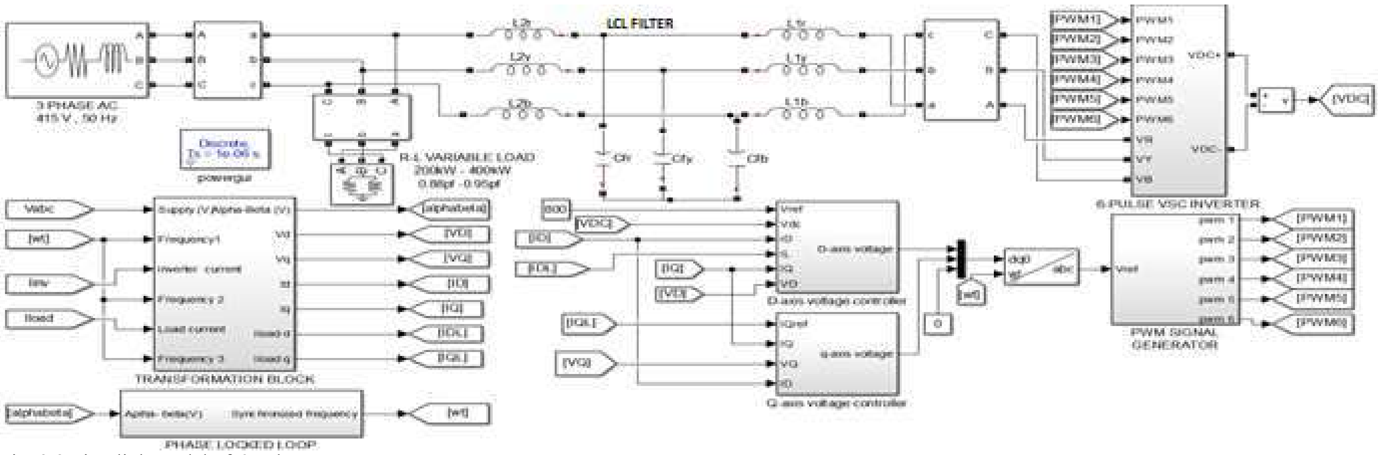

Fig. 3.2 Simulink model of 6-pulse STATCOM

2. Transformation block:

This transformation block shown in Fig. 3.2 receives voltage and current values of AC supply and load, and using the synchronous frequency generated by the PL loop, it produces instantaneous quadrature and direct axis voltages and currents based on the Park's and Clarke's transformation.

3. Control Circuit:

The control circuit is designed based on an indirect current control approach and instantaneous PQ theory principle. Revised d-axis and q-axis voltages are calculated using two controller circuits viz. direct and quadrature axis voltage controllers as shown in Fig.3.3 and Fig.3.4. The voltage controller compares the instantaneous voltage of the DC – link capacitor with a reference value set at 800V. The error is amplified by a tuned PI controller which is then fed into the (ID) direct axis current controller and compared with source and load ID current; this error is amplified by PI block and further undergoes signal conditioning to produce revised d-axis voltage. The current measurement block compares the instantaneous q-axis current with the reference load q-axis current which is modified and amplified to generate the revised q- axis voltage.

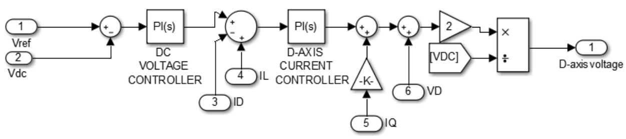

Fig.3.3. D-axis voltage controller circuit design

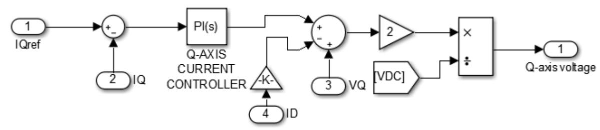

Fig.3.4. Q-axis voltage controller circuit design

4. Pulse Width Modulation Block:

The 'sine-triangle' method, in which a triangle waveform is superimposed on reference three-phase sinusoidal waveforms, is used. The switches are triggered once the carrier triangle waveform crosses the reference sinusoidal waveform, this block uses the revised d-q voltages to produce the revised 3- phase reference voltages which are used to generate PWM gate pulses fed to the IGBT switches of D-STATCOM [5].

IV. Result And Discussion

Fig.4.1 exhibits the quantum of reactive power compensation provided by the proposed D-STATCOM corresponding to R-L loads of 200kW, 300 kW and 400kW with its power factors ranging from 0.9 to 0.95.

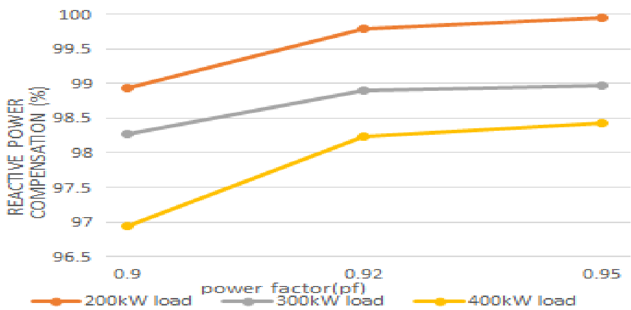

Fig. 4.1. Reactive power compensation at various R-L loads

It is noted that the D-STATCOM compensates effectively the load reactive power requirement at different load power factors and the quantum of compensation is given in Table-II.

Fig 4.2 explains the TDD characteristics at various R-L loads and it is observed that the system design fairly eliminates current harmonics at high loads and low power factors with TDD values ranging within acceptable level [20] from 2.99% to 4.6%.

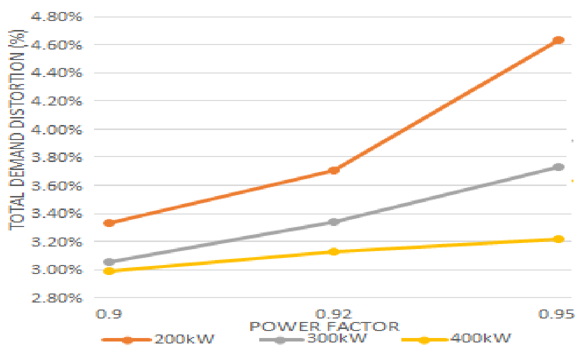

Fig.4.2. Current THD at various R-L loads

The harmonics reduction happens to be due to the LCL filter which enables to reduce the dominant 5th and 7th harmonics as shown in Fig 4.3. The TDD is 2.99% at 400kW (0.9 pf) whereas without the filter, TDD surges to 115.71% . The LCL therefore reduces TDD by approximately 97.4%. The reduction in 5th and 7th order harmonics are mentioned in Table-III at various loads .

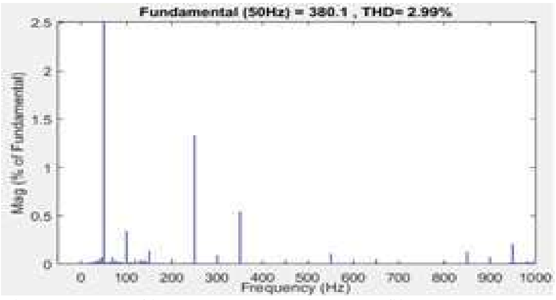

Fig. 4.3. TDD of inverter current using LCL filter

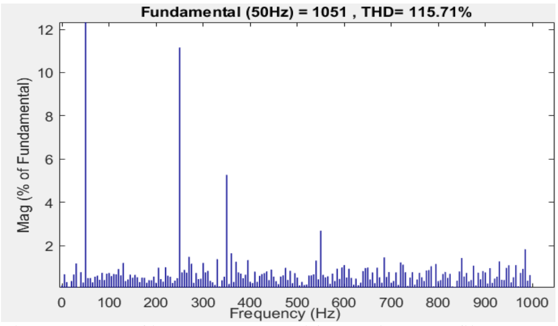

Fig. 4.4. TDD of inverter current without using LCL filter

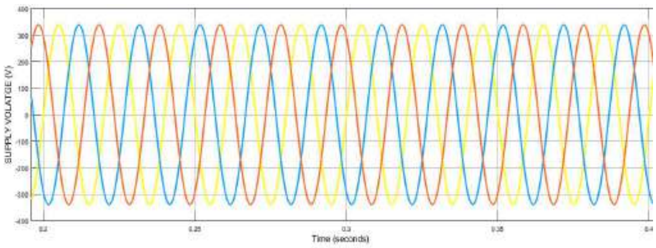

Fig. 4.5. Three phase supply voltage waveforms (V_{abc})

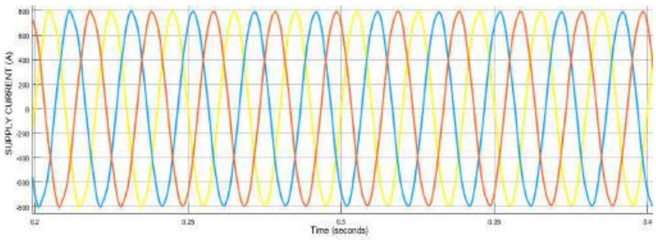

Fig. 4.6. Three phase supply current waveform (I_{abc})

Fig 4.5 is the three-phase voltage waveform of supply voltage which attains a peak value at 338V. Fig 4.6 explains the three phase current waveforms which attains peak value of 800A and is nearly in phase with supply voltage.

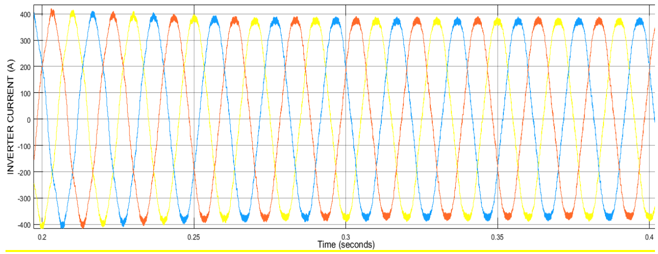

Fig. 4.7. Three phase converter current waveform(I_{inv})

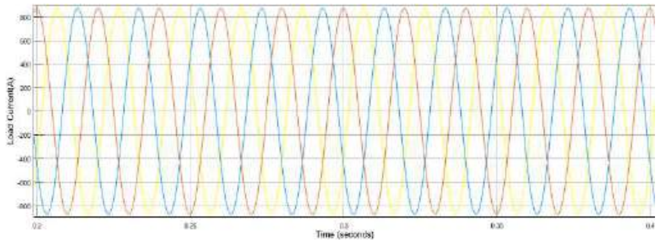

Fig. 4.8. Three phase load current waveform (I_{Load})

The converter current waveform shown in Fig 4.7 attains steady state at approximately 0.27s with steady state value of 390A. From Fig 4.8, it is observed the proposed D-STATCOM operates at 0.9 pf; I_{inv} lags I_{Load} by a very small margin as observed at time intervals 0.2s and 0.25s.

The DC voltage waveform shown in Fig 4.9 attains an overshoot of 1620V at 12ms and settles at approximately 0.23s at 800V. The ripple factor of this waveform is [(804-796)/800] *100 = 1%.

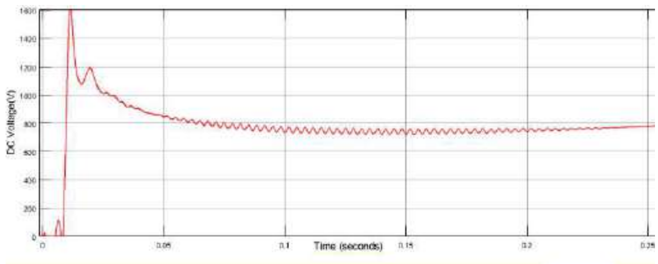

Fig 4.9. DC Voltage waveform (V_{DC})

Fig 4.10 displays exclusively the three-phase voltage waveform of the 6-pulse IGBT-VSC based D-STATCOM operating at switching frequency of 10kHz. The gate signals are generated from Sinusoidal Pulse Signal Generator, and the voltage waveform settles at approximately 0.23s at 521V. Due to almost negligible reactance between converter and the source, the waveform is nearly in phase with the supply voltage.

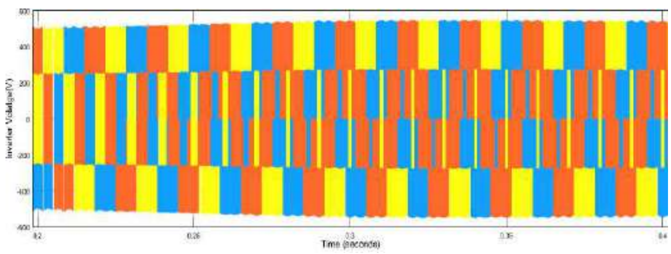

Fig. 4.10. Three phase converter voltage waveforms (V_{inv})

The active (P) and reactive (Q) power components in respect of d- axis and q-axis voltage and current are defined by the following equations:

$$P = \frac{3}{2}(V_d I_d + V_q I_q) \quad (4.1)$$

$$Q = \frac{3}{2}(V_q I_d - V_d I_q) \quad (4.2)$$

Fig 4.11 shows the d-axis current component which is approximately zero at steady state. The q-axis current waveforms as depicted in Fig 4.12, attains steady state value of 400A at 0.21s. The d-axis voltage waveform attains a steady state value of -338V in 2.5ms as indicated in Fig 4.13 (since the load is inductive and D-STATCOM shall be supplying reactive power). The q-axis voltage waveform settles to zero in 3ms as displayed in Fig 4.14 indicating thereby the fast response of the circuit to attain steady state in about one cycle (20ms) [15].

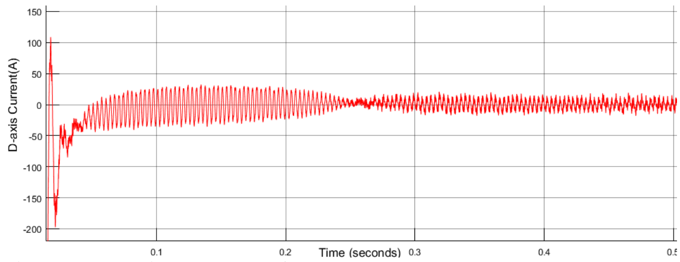

Fig. 4.11. D-axis current waveform

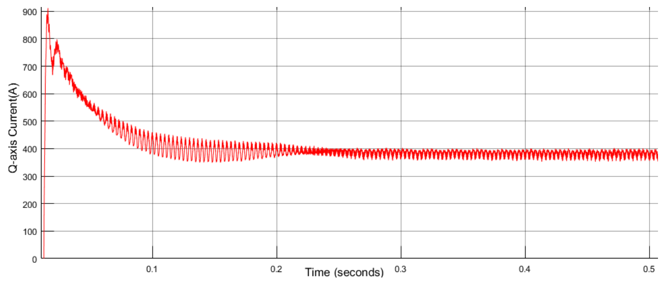

Fig. 4.12. Q-axis current waveform

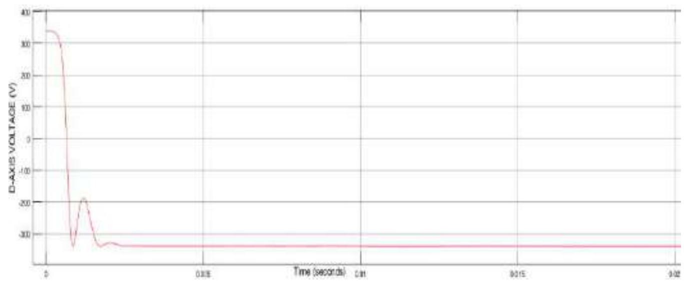

Fig. 4.13. D-axis voltage waveform

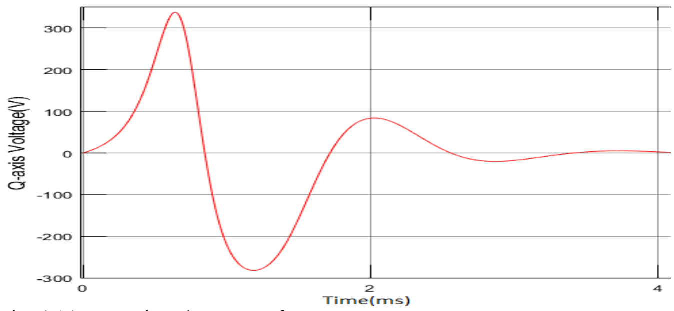

Fig. 4.14. Q-axis voltage waveform

TABLE I. DESIGN PARAMETERS OF A STATCOM

DEVICE	PARAMETERS	VALUES
SOURCE	Source volatge	415V
	Configuration	Y type
	Source resistance	1 µΩ
	Source inductance	1 µH
	Phase angle	0 degrees
	System frequency	50 Hz
CONVERTER	Power switch internal resistance	1mΩ
	Snubber resistance	1MΩ
	Switching frequency	10kHz
	Capacitor rating	Two 4260µF in series
	Capacitor resistance	1mΩ
FILTER	L_1	500 µH
	L_2	272 µH
	C_f	100 µF
	f_{res}(Hz)	1200Hz
PI CONTROLLER GAINS	DC VOLTAGE CONTROLLER (K_P,K_I)	(5,200)
	OUTPUT CURRENT CONTROLLER (K_P,K_I)	(25,500)
	INPUT Q-AXIS CURRENT CONTROLLER (K_P,K_I)	(25,500)

TABLE II. TABULAR PRESENTATION OF SIMULATION RESULTS

LOAD DEMAND (kW)	POWER FACTOR (p.f)	Q SUPPLIED BY STATCOM (kVAR)	PERCENTAGE COMPENSATION (%)	CURRENT TDD (%)
200kW	0.90	95.83	98.932	3.33%
	0.92	85.02	99.788	3.71%
	0.95	65.70	99.944	4.64%
300kW	0.90	142.80	98.280	3.05%
	0.92	126.39	98.897	3.34%
	0.95	97.59	98.971	3.73%
400kW	0.90	187.79	96.934	2.99%
	0.92	167.40	98.240	3.13%
	0.95	129.40	98.422	3.22%

TABLE III. TABULAR PRESENTATION OF HARMONICS WITH AND WITHOUT LCL FILTER AT VARIOUS LOADS

LOAD (kW)	POWER FACTOR (p.f)	WITH LCL FILTER			WITHOUT LCL FILTER		
		TDD	5TH Harm	7th Harm.	TDD	5TH Harm.	7TH Harm.
200kW	0.9	3.33%	0.07%	0.145 %	164.55 %	21%	11%
	0.95	4.64%	0.4%	0.25%	169.68	22%	12%
300kW	0.9	3.05%	0.8%	0.5%	131.33	15%	7%
	0.95	3.73%	1.5%	0.7%	135.63	16%	8%
400kW	0.9	2.99%	1.4%	0.55%	115.71 %	11%	5%
	0.95	3.22%	1.8%	0.8%	119.86 %	12%	6%

V. CONCLUSION

This paper has provided a simple approach to design and modeling of ± 200 kVAr D-Stacom using 6-pulse IGBT based VSC triggered with 10kHz PWM gate signals, and use of a low pass LCL filter. The device has been simulated in MATLAB/Simulink platform for reactive power compensation to the varying inductive loads. The results validate the fast response of the compensator for load reactive power balancing in electrical network. With the proposed design of the LCL filter and the compensator, the current TDD level has also been maintained as stipulated in IEEE-519 standards [20]. A prototype development of the proposed model can be undertaken and tested for validation as next phase of work. Further scope of improvement in the performance of STATCOM can be studied and modeled through multi-staging converter topologies and self-adaptive controllers like AI controller for versatile applications in transmission and distribution networks.

REFERENCES

[1] L. G. N.G. HINGORANI, *UNDERSTANDING FACTS CONCEPTS AND TECHNOLOGIES OF FLEXIBLE AC TRANSMISSION SYSTEMS*, vol. 6, no. 11. 1967.

[2] G. Gupta, W. Fritz, and M. T. E. Kahn, "A comprehensive review of DSTATCOM: Control and compensation strategies," *Int. J. Appl. Eng. Res.*, vol. 12, no. 12, pp. 3387–3393, 2017.

[3] H. A. Hassan, Z. H. Osman, and A. E.-A. Lasheen, "Sizing of STATCOM to Enhance Voltage Stability of Power Systems for Normal and Contingency Cases," *Smart Grid Renew. Energy*, vol. 05, no. 01, pp. 8–18, 2014, doi: 10.4236/sgre.2014.51002.

[4] Aishvarya Narain and S. K. Srivastava, "An Overview of Facts Devices used for Reactive Power Compensation Techniques," *Int. J. Eng. Res.*, vol. V4, no. 12, pp. 81–85, 2015, doi: 10.17577/ijertv4is120071.

[5] K. Wang and M. L. Crow, *Modern flexible AC transmission system (FACTS) devices*. Woodhead Publishing Limited, 2013.

[6] J. Liu, J. Chen, and Z. Qian, "Comparative analysis of FACTS devices based on the comprehensive evaluation index system," *MATEC Web Conf.*, vol. 95, pp. 1–5, 2017, doi: 10.1051/matecconf/20179515002.

[7] B. Oum, E. Fadhel, and M. Fellah, "Theory , Modelling and Control of FACTS devices THEORY , Modelling and Control of FACTS devices . Laboratoire ICEPS (Intelligent Control & Electrical Power Systems)," no. February, 2015.

[8] A. ÇETİN, "Design and implementation of a voltage source converter based statcom for reactive power compensation and harmonic filtering," *Pravoslavie.ru*, no. April, 2007.

[9] S. Kumar, "controllers using Evolutionary Techniques," pp. 962–965, 2020.

[10] B. S. Pali, S. Bhowmick, and N. Kumar, "Newton-Raphson power flow models of static VAR compensator," *India Int. Conf. Power Electron. IICPE*, pp. 9–13, 2012, doi: 10.1109/IICPE.2012.6450443.

[11] T. Navpreet *et al.*, "Voltage Source Converters as the building block of HVDC and FACTS Technology in Power Transmission System: A Simulation based Approach," *Pelagia Res. Libr. Adv. Appl. Sci. Res.*, vol. 3, no. 5, pp. 3263–3278, 2012, [Online]. Available: www.pelagiaresearchlibrary.com.

[12] S. Bernet, R. Teichmann, S. Member, A. Zuckerberger, and P. K. Steimer, "Comparison of High-Power IGBT ' s and Hard-Driven GTO ' s for High-Power Inverters," vol. 35, no. 2, pp. 487–495, 1999.

[13] T. Mittal, N. S. Tung, A. D. Diwan, and K. Janardhana, "STATCOM Analysis for improving Power Quality Constraints - A Literature Survey," vol. 1, no. 1, pp. 1–10, 2012.

[14] A. Mokhtari, F. Z. Gherbi, C. Mokhtar, and D. E. Kamel, "Study , analysis and simulation of a static compensator D-STATCOM for distribution systems of electric power," *Leonardo J. Sci.*, no. 25, pp. 117–130, 2014.

[15] J. K. Bhutto and R. Bana, "Design of the Dstatcom and Analysis of the Controllers for Power Quality Improvement," pp. 24–37.

[16] C. Wang, X. Yin, M. Wen, J. Liu, Q. Xiong, and B. Zhang, "Structure and parameters design of output LC filter in D-STATCOM," *2010 Int. Conf. Power Syst. Technol. Technol. Innov. Mak. Power Grid Smarter, POWERCON2010*, pp. 1–6, 2010, doi: 10.1109/POWERCON.2010.5666674.

[17] K. S. Rao and R. Mishra, "Comparative study of P, PI and PID controller for speed control of VSI-fed induction motor," vol. 2, no. 2, pp. 2740–2744, 2014, [Online]. Available: http://www.ijedr.org/papers/IJEDR1402230.pdf.

[18] A. Oudalov, R. Cherkaoui, and A. J. Germond, "Power Flow Control By Multiple Series Facts Devices," *System*.

[19] M. Dursun and M. K. Dosoglu, "LCL Filter Design for Grid Connected Three-Phase Inverter," *ISMSIT 2018 - 2nd Int. Symp. Multidiscip. Stud. Innov. Technol. Proc.*, no. 3, pp. 2018–2021, 2018, doi: 10.1109/ISMSIT.2018.8567054.

[20] "IEEE Recommended Practice and Requirements for Harmonic Control in Electric Power Systems," in IEEE Std 519-2014 (Revision of IEEE Std 519-1992) , vol., no., pp.1-29, 11 June 2014, doi: 10.1109/IEEESTD.2014.6826459.

Solar PV based Forest Fire Detection and Monitoring using Zigbee Protocol

Vidushi Singh
Electrical Engineering Department
Delhi Technological University
Delhi, India
vidushisinghmay27@gmail.com

Rekha
Electrical Engineering Department
Delhi Technological University
Delhi,India
rekhamina19@gmail.com

Radheshyam Saha
Electrical Engineering Department
Delhi Technological University
Delhi,India
rshahacno@yahoo.com

V.R.Vanjari
Electrical Engineering Department
Delhi Technological University
Delhi , India
venkat.vr90@gmail.com

***Abstract*—Forest Fire is one of the most frequent types of natural disasters. It represents a significant danger to not only the environment but to human existence as well. Therefore, its early detection is of prime importance. The scope of application of traditional fire detection systems is restricted by a variety of factors such as financial, material resource, and trained labor constraints which reduces its efficacy in fire detection. This paper deals with counteracting the disadvantages associated with traditional fire detection systems by employing a Zigbee-based Wireless Sensor Network system that detects forest fires and notifies the concerned authorities using GSM. It consists of two main modules. First, the Transmitter-End module, located in the forest area which records the real-time temperature and gas value parameters using an LM35 temperature sensor and an MQ-2 smoke sensor. Since grid supply at the forest area is inaccessible a 12V, 5W photo-voltaic panel is used to power the transmitter-end module. Second, the Receiver-End module which is located at the control center. This system can monitor and transmit the temperature and gas values to the control center and send a text alert if the recorded value exceeds the threshold value.**

***Keywords*—Zigbee, GSM, fire detection, temperature, smoke, forest fire, WSN**

I. INTRODUCTION

Fire is a natural phenomenon that has proved to be crucial for the survival of mankind. Man has relied on it for centuries for their everyday tasks and utilized it as a source of fuel for cooking, heating, and light. However uncontrolled fire can pose a major threat to human existence and property, in the form of forest fires, household fire accidents, etc. Globally, 9 mi1lion fire incidents and 1.2 1akh mortalities were recorded according to a 195-nation ana1ysis by G1oba1 Disease Burden, and out of these incidents, India recorded 1.6 mi11ion fires and 27,027 mortalities, making every 5th fire-re1ated death in the wor1d occurring in India [1].

Therefore, it is essential to have a fire detection system that can detect fires and alert the concerned authorities. A fire detection system provides an early warning signal for a fire outbreak after detecting a fire. At present patrolling, surveillance, observation from watchtowers, and satellite monitoring serve as prevention methods used for the detection of forest fires [2]. Patrolling and observation via watchtowers is easy and viable but multiple limitations are associated with it due to financial, material resource, and trained labour constraints. Similarly, satellite monitoring has restricted application due to its long scanning cycles, high cost, and poor resolutions [3]. To equilibrate these limitations associated with traditional forest fire monitoring systems, a Zigbee-based WSN (Wireless Sensor Network) system has been proposed. Zigbee is a 1ow-power, 1ow-cost specification used for wireless communication [4]. This system can monitor and transmit real-time temperature and gas values to the monitoring centre and send an alert if the recorded value exceeds the threshold value [5]. The proposed system uses an LM35 Temperature sensor and an MQ-2 smoke sensor to monitor the real-time temperature and gas value parameters. GSM and Zigbee are used for wireless communication between the transmitter-end module and the receiver-end module.

I. LITERATURE SURVEY

Innumerab1e so1utions are proposed and app1ied for so1ving the prob1ems associated with forest fires. The most usual systems utilized in the fie1d work are video survei11ance structures. Video cameras are sensitive to smoke and are most

effective in the daytime [2]. Fire-sensitive cameras in the dark, the usage of IR thermal imaging cameras for warmth flux detection, and the usage of backscattering of laser light are used to locate the smoke particles. This fire alert gadget has a few limitations due to environmental situations like dirt particles, mist, and shadows [3]. Another technique is a computerized photo capturing of fires in the woodland. Capturing is often finished through the cameras which can be located on top of towers. [4] Proposed a system where a coverage view of the forest was offered, and then the captured photos are processed by the usage of a program or MATLAB simulation and matched with references taken at starting stage. This alert gadget has a predicament of fake warning rates and visible cameras mounted on watchtowers are of excessive cost. Another technique of fire detection is through the usage of a satellite. The base station collects the data despatched through the satellite and runs an algorithm to acknowledge the facts. An Advanced Very High-Resolution Radiometer (AVHRR) is used to detect the presence of Hot Spots after the raw data from the satellite(s) is processed. This system is greatly affected by the presence of clouds [2].
[5] proposed, a forest fire closed-circuit through the usage of a Wi-Fi sensor network. WSN detects humidity and the software analyses the accumulated information. In this methodology, there are a few losses of data throughout the communication. According to the paper published by J. Zhang, W. Li, N. Han, and J. Kan, a proposal for a fire detection approach that's primarily based on effective device knowledge and deep knowledge of algorithms was introduced [6]. Both sensor data, as well as image data records, were used for forest fire prevention. [7] proposed an implementation technique of intelligent smoke alarm devices, such as sensor network, classification algorithm, and visible interface. Then, the trouble of low precision of conventional smoke alarms is evident. The experimental consequences display that, based on the proposed intelligent smoke alarm device, the air conditions and the chance of fake alarms may be reduced. In the future, they can try and discover extra varieties of smog withinside the equal sensor device.

II. ZIGBEE

ZigBee is an IEEE 802.15.4 based, low-power, low-information rate supporting remote systems administration standard that is essentially utilized in two-path correspondences between sensors and control framework [8]. A modest survey on this technology[8-23] has been carried out in the context of the propose research work. Briefly, it has a short correspondence range of 10 to 100 meters similar to Wi-Fi and Bluetooth. ZigBee Technology upholds the movement of basic information, unlike Wi-Fi and Bluetooth which supports the exchange of complex construction like media, programming, and so forth. It upholds a low information pace of around 250 kbps [9]. The working frequencies for the Zigbee protocol are 868 MHz, 915 MHz, and 2.4 GHz. This technology is utilized principally for applications that require low force, ease, and low information rate. This network protocol observes IEEE 802.15.4 norms for Physical (PHY) and Medium Access Control (MAC) layers, alongside its Network (NWK) and Application (APL) layers (Fig.1) [10].

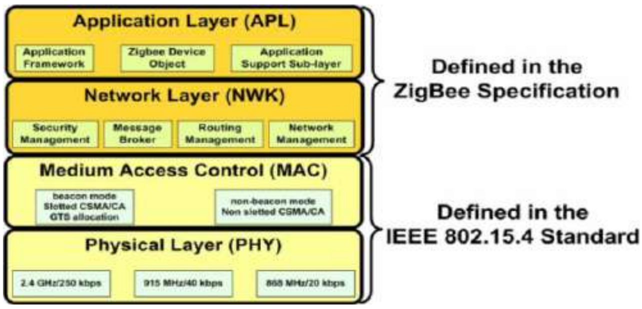

Fig. 1 Zigbee architecture

Each layer is having the functionalities as explained below:

1. Physical layer: It is the most minimal convention layer, which is answerable for managing and actuating the radio - handset, and furthermore for choosing and checking the channel recurrence [11]. It is likewise answerable to radio gadgets for correspondence. Correspondence of information or orders is finished by utilizing Packets. Each PHY Packet comprises a Synchronization Header (SHR) (responsible for receiver synchronization), Physical Header (PHR) (accommodates data about Frame length), and PHY payload (given by upper layers as a casing and incorporates information or order).

2. Medium Access Control or MAC Layer: It goes about as an interface between the Physical Layer and the Network layers. It is answerable for the age of Beacons and the synchronization of gadgets in the Beacon-empowered organization [12]. A MAC frame can be a Beacon Frame (utilized by the Coordinator to send Beacons), Data Frame, Acknowledge Frame, or Command Frame. It comprises a MAC Header (accommodates data regarding security and), Variable-length size MAC Payload (contains information or order), and a MAC Footer (accommodates 16-digit Frame check arrangement for information confirmation) [10].

3. Network Layer: This layer associates the Application layer with the MAC layer. It deals with network development and routing. It sets up another network and chooses the network topology. The NWK frame comprises the NWK Header and NWK Payload. The Header contains data concerning network level control. The NWK Payload contains the Application sublayer outline [13][14].

4. Application Support Sub Layer: It uses Application Support Data Entity and Application Support Management Entity to provide a bunch of services to the application and network layers. This information is received via separate Service Access Points (SAP) [15].

5. Application Layer: It is the highest layer in the network. It is liable for facilitating the application objects that hold client applications and ZigBee Device Objects (ZDOs). A solitary ZigBee gadget can accommodate up to 240 application objects that controls and deals with the convention layers [10]. Every application item can comprise one application profile or program, created by the client or the ZigBee collusion. The application profile is answerable for the transmission and gathering of information in the organization. The kind of gadgets and capacity of every gadget is characterized in an application profile [13]. The ZDOs go about as an interface amongst application objects, gadget profiles, and the application sub-layer.

ZigBee is exceedingly better when compared to some other advanced technologies like Bluetooth, Bluetooth LE, Wi-Fi, and Home RF. Comparison based on different technical aspects between Zigbee and these technologies[16-17] has been given in Table1.

Table. 1 Comparison of Zigbee with other technologies

Parameters	ZigBee	Bluetooth	BLE	Wi-Fi	Home RF
Frequency Band	2.4GHz/ 915MHz/ 865MHz	2.4GHz	2.4GHz	2.4GHz	2.4GHz
Maximum bit rate	250kb/s	1Mb/s		1Mb/s	1.6Mb/s
Power	36.9mW	215mW	10mW	835mw	835mw
Coverage Area (m)	100 (indoors)	10	10	50	50
Network Nodes	65,000	80	Limited by the application	50	127
Complicity	Simple	Complex	Complex	Very Complex	Very Complex
Standard	IEEE 802.15.4	IEEE 802.15.1	IEEE 802.15.1	IEEE 802.1	IEEE 802.11
Channel Bandwidth	2MHz	1MHz	1MHz	22MHz	22MHz
Network Topologies	P2P,tree,star,mesh	Scatternet	Star-bus	Point-to-hub	Point-to-hub

III. SYSTEM DEVELOPMENT

The proposed system consists of two modules: First is the Transmitter-End module which is located at the forest area to provide real-time temperature and gas value parameters recorded by the sensors and, second is the Receiver-End module which is located at the control center to monitor these parameters [18]. The Transmitter-End module (Fig. 2 and 5) is the primary unit of this system. It consists of an LM35 Temperature sensor and an MQ-2 smoke sensor to monitor the environmental conditions at the site [3]. A 16x2 LCD is used to display the recorded parameters. If the recorded parameters exceed the threshold values, a text alert and buzzer are used to alert the concerned authorities. Zigbee transceiver and SIM 800 GSM module are connected to the transmitter-end module to establish wireless communication [15]. A 12V, 5W Photo-voltaic solar panel is used for fulfilling the energy requirements as the transmitter-end module is placed at the forest area where getting power supply from the grid is difficult.

The Receiver-End module (Fig. 3 and 6) consists of a Zigbee transceiver and a 16x2 LCD to display the parameters recorded by the LM35 and MQ-2 sensors at the transmitter-end. An ATmega328P microcontroller is used as the processing unit for both transmitter-end and receiver-end modules.

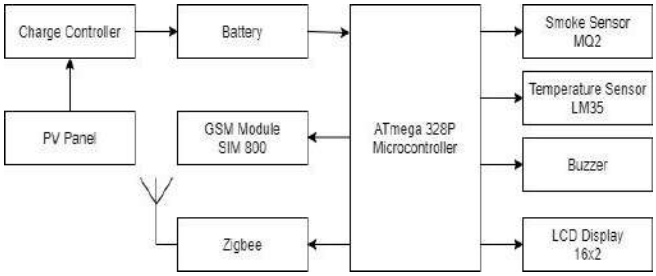

Fig. 2 Block diagram of Transmitter-End

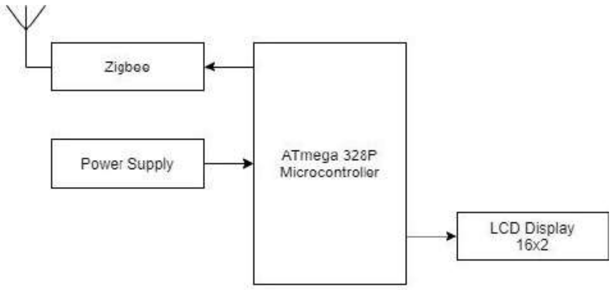

Fig. 3 Block diagram of Receiver-End

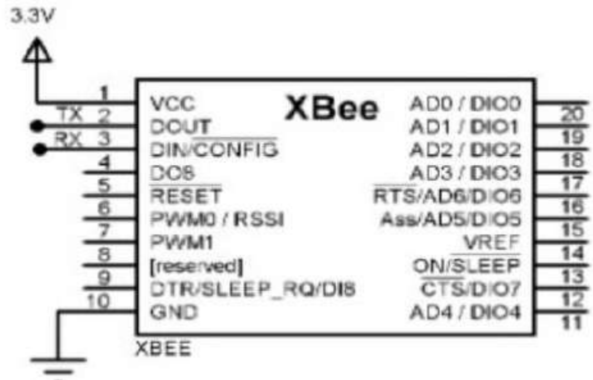

Fig. 4 Zigbee Pin configuration

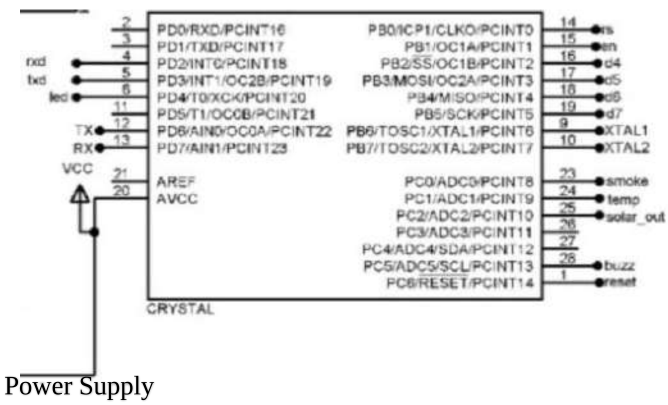

Fig. 5 Atmega328P microcontroller Pin configuration

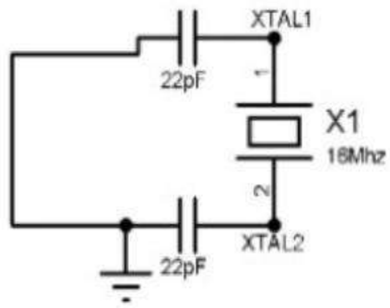

Fig. 6 Crystal Oscillator

Fig4 and fig 5 shows the pin configuration of Zigbee and Atmega 328P microcontroller respectively. The power supply is connected to the pin no.20 of the microcontroller as shown in fig 5. Fig 6show the crystal oscillator, the XTAL1 and XTAL2 of the crystal oscillator are connected to PB6 and PB7 pins respectively. It acts as an external source to provide the clock frequency.

As mentioned, the proposed system alerts the authorized user using a text alert and buzzer if the temperature and gas values recorded by the LM35 and MQ-2 sensors exceed the threshold values. The threshold temperature value for the temperature sensor is kept at >= 50°C and the concentration range for the smoke sensor is from 200ppm to 10000ppm as shown in Fig.7 .

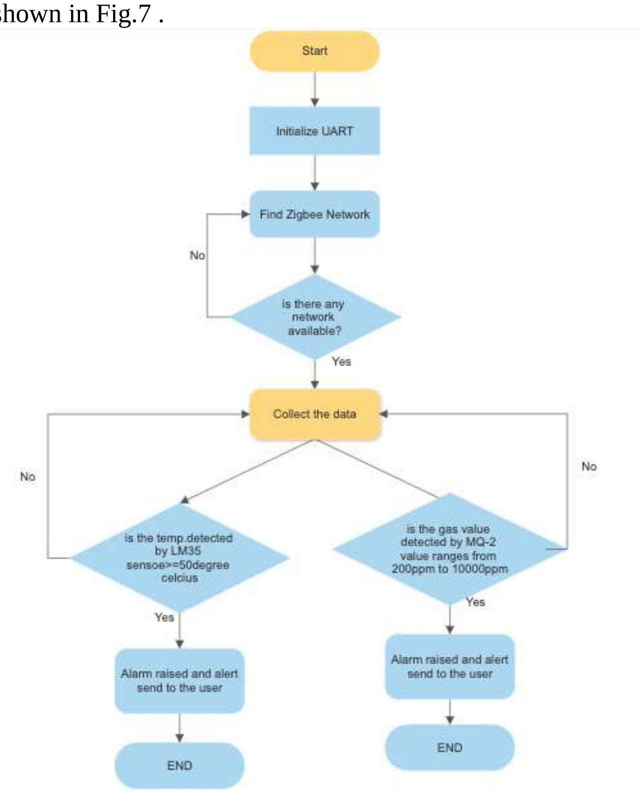

Fig. 7 System Flowchart

Based on the flow chart the programming has been done in the microcontroller.

IV. System Design and Hardware Implementation

There are three crucial stages involved in the proposed Zigbee-based fire detection and alert system: Sensing, Routing, and Communication. The MQ-2 smoke sensor and LM35 temperature sensor are used for sensing the physical change in the environment. The MQ-2 sensor device is created from alumina and features a coating of tin dioxide (SnO_2) which is very sensitive toward flammable or combustible gases [20]. If a flammable or combustible gas exists, the sensor's conductivity rises corresponding to the rise in the concentration of combustible gases at the detection site. This sensor has a very high sensitivity toward fuel, methane, LPG, smoke, alcohol, carbon monoxide, and hydrogen gas [21]. It is connected to the ADC0 pin of the microcontroller.

Table.2 List of major Hardware Equipments

Hardware	Specifications
Solar Panel	12W,5V
Battery	12V,1.2Ah
Atmega328P microcontroller	32k,8-bit ,28 pin
Crystal Oscillator	16MHz
ZigBee	2.4GHz
LM35 Temperature Sensor	Range from −55°C to 150°C
MQ2 Smoke Sensor	5V DC & draws around800mW,Concentration range from 200-10000ppm
GSM	SIM 800
7805- Voltage Regulator	Output regulated +5V
IN5408 Diode	Current Capacity of 3A

Another key sensor present within the project is the temperature sensor LM35, which is very sensitive and responsive to temperature change (Fig. 5). This sensor measures the temperature as an electrical output corresponding to the temperature in degree Celsius (°C)[22]. This sensor supersedes other thermocouples as it generates a high output voltage that need not be amplified. The output voltage produced by LM35 is proportional to the temperature in degree Celsius (°C) with a scale factor of 0.01V/ °C. It is connected to the ADC1 pin of the microcontroller. These two sensors help in the detection of fire by recording the temperature value, gas value and transmitting the acquired data via Zigbee [23]. The Zigbee Module used in the project is a ZigBee Series two Module that performs the function of serial communication through a wireless medium. It is connected to the PD6 and PD7 pins of the ATmega328P microcontroller. The ATmega328P is an AVR architecture-based 32K 8-bit microcontroller that executes multiple instructions in a single clock cycle providing a throughput of almost 20 MIPS at 20MHz. The ATmega328P comes in a PDIP 28 pin package and is suitable for use on 28 pins AVR

Development Board. It is used because of its low power consumption and ease of availability. The XTAL1 and XTAL2 of the crystal oscillator are connected to PB6 and PB7 pins respectively. It acts as an external source to provide the clock frequency. If the system detects a rise in temperature or any gas leakage, it sends information to the authorized user of this event through a Zigbee wireless interface to the receiver-end module and a text alert to the registered mobile number using SIM 800 GSM module[9][14]. Global System for Mobile communication (GSM) consists of transmission and reception pins. It accepts a SIM card to perform functions like calling, sending or receiving a message for communication over the network. It is interfaced with the ATmega328P microcontroller through the PD2 and PD3 pins. GSM module features an extensive coverage and is extremely cost-effective,

This project utilizes solar energy for fulfilling the energy requirements at the transmitter-end module which is located in the forest area [19]. Since grid supply at the forest area is inaccessible a 12V, 5W photo-voltaic panel is used to power the module. This PV has V_{mpp} and I_{mpp} of 12V and 0.42A,and V_{oc} and I_{sc} of 14.4V and 0.46A respectively. A 12V, 1.2 Ah lead-acid battery is used so that the system runs efficiently even when direct sunlight is unavailable. An LM358 dual op-amp is used as a comparator for the voltage divider circuit. It has a range of 3V-32V for a single power supply and ±1.5V to ±16V for a dual power supply. To ensure that the current flows only in one direction a 1N5408 Diode is used in the circuit. It has a maximum current carrying capacity of 3A. For all the components to work properly a constant supply is required. Therefore, a voltage regulator is used for a constant and continuous supply of voltage. By using a 7805- voltage regulator, 5 V constant output voltage is supplied which is connected to the pin 20(AVCC) of the 328P microcontroller.

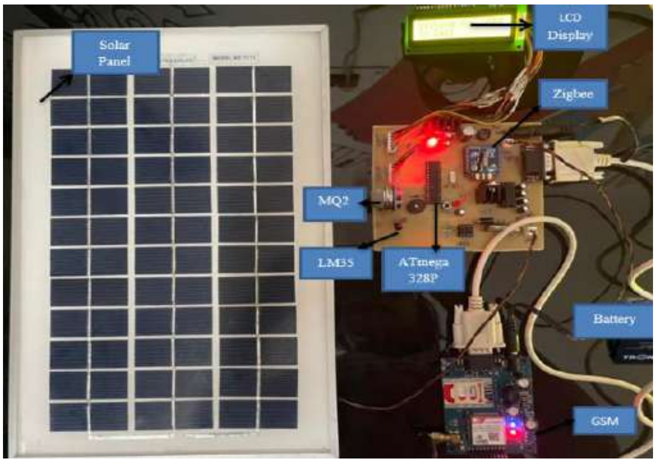

Fig. 8 Transmitter-End Module

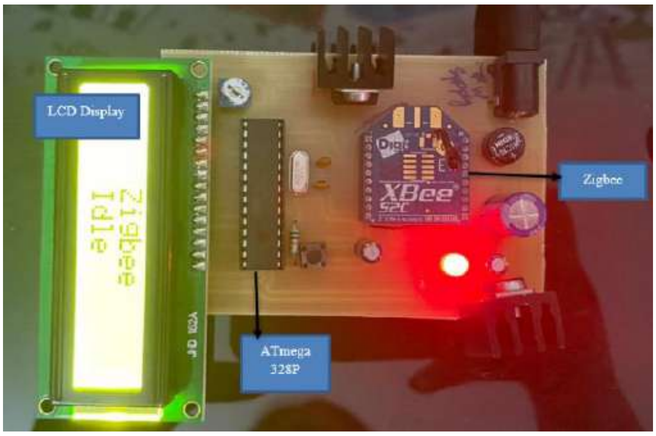

Fig. 9 Receiver-End Module

V. Results and Observations

In our project we are using solar panel to provide supply to the controlling unit at the forest side. Since in a forest the electrical energy may be critical and sun is a big source of energy during the day time. In a day time battery is charged as well as it is used as a supply for controlling unit. . An LM358 dual op-amp is used as a comparator for the voltage divider circuit. It has a range of 3V-32V for a single power supply and ±1.5V to ±16V for a dual power supply. To ensure that the current flows only in one direction a 1N5408 Diode is used in the circuit. It has a maximum current carrying capacity of 3A. For all the components to work properly a constant supply is required. Therefore, a voltage regulator is used for a constant and continuous supply of voltage. By using a 7805- voltage regulator, 5 V constant output voltage is supplied which is connected to the pin 20(AVCC) of the 328P microcontroller. The temperature and smoke sensor are connected to the pin 24 and 23 of 328P microcontroller respectively. The analog output voltage provided by the sensor changes in proportional to the concentration of smoke/gas(200-10000ppm) and similarly the analog output voltage provided by the sensor is connected to the range of temperature. If the system detects a rise in temperature or any gas leakage, it sends information to the authorized user of this event through a Zigbee wireless interface to the receiver-end module and a text alert to the registered mobile number using SIM 800 GSM module.
The wireless transmission of alert signals using Zigbee from the transmitter-end module to the receiver-end module was experimented with up to 50m. Since signal obstruction in the forest area would be limited, the system is expected to work efficiently for larger distances. There should be minimum network coverage for GSM modules to work properly and send an SMS. When a fire is detected at the transmitter-end module, the buzzer rings, and LCD display’s a message as shown in Fig. 10and Fig.11.

Fig. 10 Tx LCD Display (fire alert)

Fig. 11 Rx LCD Display (fire alert)

Similarly, when a combustible gas is detected, a message is displayed at the LCD at both the transmitter-end (Fig. 10) and receiver-end modules (Fig. 11). Simultaneously a text alert via SMS is sent to the registered mobile number (Fig. 14).

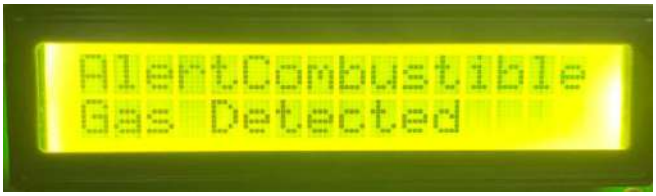

Fig. 12 Transmitter-end x LCD Display (gas alert)

Fig. 13 Receiver-end LCD Display (gas alert)

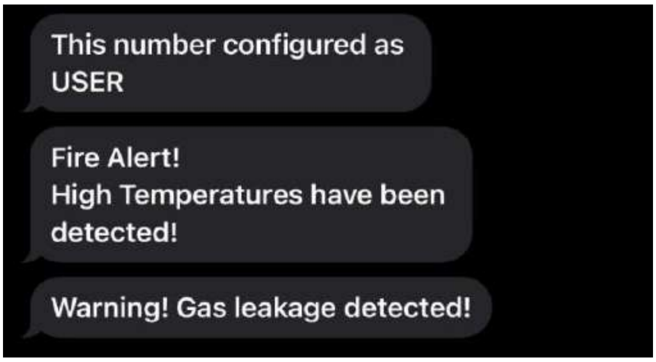

Fig. 14 Text alert messages.

VI. CONCLUSION

In this paper ,a new design and imp1ementation of a solar powered system for ear1y detection of forest fire and its monitoring with regard to temperature and smoke sensing has been illustrated. The proposed system overcomes the shortcomings of the traditiona1 techno1ogies used for this purpose. Zigbee and GSM technologies are used for ensuring reliable communication between the transmitter end and receiver end networks. This system will be very useful where grid supply is absent, because of the use of so1ar energy to overcome the power supply requirements. The proposed system has certain advantages in comparison to traditional techniques such as high durability, low cost, high network capacity, ease of installation and maintenance, etc.

The current system can be expanded by using a mesh network of multiple sensor nodes to cover a wide area of forest for fire detection and monitoring. Furthermore, the system can be made more efficient by interfacing other sensors such as humidity sensors and pressure sensors so that additional environmental conditions can be monitored. An intricate monitoring system can be developed where users can monitor real-time parameters and perform remote actions.

REFERENCES

[1] S. L. James *et al.*, "Global, regional, and national incidence, prevalence, and years lived with disability for 354 Diseases and Injuries for 195 countries and territories, 1990-2017: A systematic analysis for the Global Burden of Disease Study 2017," *Lancet*, vol. 392, no. 10159, pp. 1789–1858, Nov. 2018.

[2] D. Stipaničev, T. Vuko, D. Kristinić, M. Štula, and L. Bodrožić, "Forest Fire Protection by Advanced Video Detection System - Croatian Experiences," *Third TIEMS Work. Improv. Disaster Manag. Syst.*, p. 10, 2006.

[3] P. Dasari, G. Krishna, J. Reddy, and A. Gudipalli, "Forest fire detection using wireless sensor networks," *Int. J. Smart Sens. Intell. Syst.*, vol. 13, no. 1, pp. 1–8, 2020.

[4] A. Losso, L. Corgnati, and G. Perona, "False alarm reduction in forest fires detection with low-cost commercial sensors," *Ital. J. Remote Sens. / Riv. Ital. di Telerilevamento*, vol. 43, no. 1, pp. 75–86, 2011.

[5] M. Y. H. M. Y. Hariyawan, A. G. A. Gunawan, and E. H. P. E. H. Putra, "Wireless Sensor Network for Forest Fire Detection," *TELKOMNIKA (Telecommunication Comput. Electron. Control.*, vol. 11, no. 3, p. 563, Sep. 2013.

[6] J. Zhang, W. Li, N. Han, and J. Kan, "Forest fire detection system based on a ZigBee wireless sensor network," *Front. For. China*, vol. 3, no. 3, pp. 369–374, Sep. 2008.

[7] Q. Wu *et al.*, "Intelligent Smoke Alarm System with Wireless Sensor Network Using ZigBee," *Wirel. Commun. Mob. Comput.*, vol. 2018, no. 2, 2018.

[8] H. Cao, X. Liang, I. Balasingham, and V. C. M. Leung, "Performance analysis of ZigBee technology for Wireless Body Area Sensor Networks," in *Lecture Notes of the Institute for Computer Sciences, Social-Informatics and Telecommunications Engineering*, 2010, vol. 28 LNICST, pp. 747–761.

[9] T. Defeng, L. Shixing, X. Wujun, and Z. Yongming, "A fire monitoring system in ZigBee wireless network," *Proc. - 2010 Int. Conf. Cyber-Enabled Distrib. Comput. Knowl. Discov. CyberC 2010*, pp. 48–51, 2010.

[10] P. Mohana and S. Radha, "Realization of MAC layer functions of ZigBee protocol stack in FPGA," *2009 Int. Conf. Control Autom. Commun. Energy Conserv. INCACEC 2009*, 2009.

[11] D. K. kumar, G. Kishore, and T. V. S. kumar, "Fire Monitoring System for Fire Detection Using ZigBee and GPRS System," *IOSR J. Electron. Commun. Eng.*, vol. 12, no. 01, pp. 23–27, 2017.

[12] P. Vidyashree and S. Pushpalatha, "The design and implementation of building fire monitoring system using zigbee-wifi gateway," *Int. Res. J. Eng. Technol.*, vol. 4, no. 7, pp. 3030–3032, 2017.

[13] C. M. Ramya, M. Shanmugaraj, and R. Prabakaran, “Study on ZigBee technology,” in *ICECT 2011 - 2011 3rd International Conference on Electronics Computer Technology*, Apr. 2011, vol. 6, pp. 297–301.

[14] S. G. Ma, “Construction of wireless fire alarm system based on ZigBee technology,” *Procedia Eng.*, vol. 11, pp. 308–313, 2011.

[15] J. K. Park and H. Seo, “ZigBee-Based Smart Fire Detector for Remote Monitoring and Control,” *Int. J. Adv. Sci. Technol.*, vol. 29, no. 3, pp. 10431–10441, 2020.

[16] X. Silvani, F. Morandini, E. Innocenti, and S. Peres, “Evaluation of a Wireless Sensor Network with Low Cost and Low Energy Consumption for Fire Detection and Monitoring,” *Fire Technol.*, vol. 51, no. 4, pp. 971–993, 2015.

[17] H. M. Jawad, R. Nordin, S. K. Gharghan, A. M. Jawad, and M. Ismail, “Energy-efficient wireless sensor networks for precision agriculture: A review,” *Sensors (Switzerland)*, vol. 17, no. 8, 2017.

[18] A. Molina-Pico, D. Cuesta-Frau, A. Araujo, J. Alejandre, and A. Rozas, “Forest Monitoring and Wildland Early Fire Detection by a Hierarchical Wireless Sensor Network,” *J. Sensors*, vol. 2016, pp. 1–8, 2016.

[19] C. Tikhe and N. Rail, “So1ar Powered Wireless Forest Fire Detection,” *Int. J. Adv. Res. Comput. Commun. Eng. ISO*, vol. 7, no. 4, pp. 80–83, 2018.

[20] P. Naik, P. Dhopte, R. Wanode, R. Kantode, and S. Nagre, “Gas Sensor Using Arduino UNO & MQ2 Sensor,” *Int. J. Adv. Res. Comput. Commun. Eng. ISO*, vol. 7, no. 3, pp. 548–550, 2007.

[21] I. K. N. Trisnawan, A. N. Jati, N. Istiqomah, and I. Wasisto, “Detection of Gas Leaks Using the MQ-2 Gas Sensor on the Autonomous Mobile Sensor,” in *2019 International Conference on Computer, Control, Informatics, and its Applications: Emerging Trends in Big Data and Artificial Intelligence, IC3INA 2019*, Oct. 2019, pp. 177–180.

[22] P.MARIAN, “LM35 Precision Centigrade Temperature Sensors General Description FIGURE 1. Basic Centigrade Temperature Sensor (+2˚C to +150˚C) FIGURE 2. Full-Range Centigrade Temperature Sensor,” 2000.

[23] H. Yang, S. Geng, L. Hou, J. Wang, X. Peng, and W. Wu, “Research of fire detecting system based on ZigBee Wireless Network,” in *Proceedings of the 2012 International Conference on Industrial Control and Electronics Engineering, ICICEE 2012*, 2012, pp. 251–253.

WORKSHOP/GIAN ATTENDED

- One Day Workshop On "Power Electronics in Smart Grid and Optimal Power Trading Mechanism", 3rd November, 2018, EED, Delhi Technological University, Delhi.
- Two days IEEE Workshop cum Exposition on " Grid Integrated Renewables & Electric Transportation", 17th & 18th December 2019 ,EED, Delhi Technological University, Delhi.
- Faculty Development Programmes,6th-10th July, 2020 on "Power Quality and Reactive Power Management", EED, Delhi Technological University …… Expert Talk on "Reactive Power Compensation and Control"
- Faculty Development Programmes, Aug 24- Aug 29 2020 on "Emerging Trends in Power Electronics and Power System" Department of Elect. Engg., O P Jindal University, Raigarh, Chattishgarh …… …… Expert Talk on " Power Electronics and Power System"
- GIAN Course on Global Initiative of Academic Networks (GIAN) courses SMART Power Flow Controller for Smart Grid Applications scheduled to be held at DELHI TECHNOLOGICAL UNIVERSITY (DTU), Dec18-22,2017.